Energy Conversion and Management 227 (2021) 113581

Contents lists available at ScienceDirect

Energy Conversion and Management

journal homepage: www.elsevier.com/locate/enconman

Design and multi-criteria optimisation of a trigeneration district energy system based on gas turbine, Kalina, and ejector cycles: Exergoeconomic and exergoenvironmental evaluation

Amir Ebrahimi-Moghadam [a,*], Mahmood Farzaneh-Gord [b], Ali Jabari Moghadam [c], Nidal H. Abu-Hamdeh [d,e], Mohammad Ali Lasemi [a], Ahmad Arabkoohsar [a], Ashkan Alimoradi [f,g,*]

[a] Department of Energy Technology, Aalborg University, Denmark
[b] Faculty of Engineering, Mechanical Engineering Department, Ferdowsi University of Mashhad, Mashhad, Iran
[c] Faculty of Mechanical Engineering, Shahrood University of Technology, Shahrood, Iran
[d] Center of Research Excellence in Renewable Energy and Power Systems, King Abdulaziz University, Jeddah 21589, Saudi Arabia
[e] Department of Mechanical Engineering, Faculty of Engineering, King Abdulaziz University, Jeddah 21511, Saudi Arabia
[f] Department for Management of Science and Technology Development, Ton Duc Thang University, Ho Chi Minh City, Vietnam
[g] Faculty of Applied Sciences, Ton Duc Thang University, Ho Chi Minh City, Vietnam

ARTICLE INFO

Keywords:
Trigeneration district energy system
Exergoeconomic analysis
Exergoenvironmental analysis
Artificial neural network
NSGA-II optimisation

ABSTRACT

A novel trigeneration district energy system (TDES) is designed and evaluated from energy, exergy, exergoeconomic, and exergoenvironmental points-of-view. By recovering the wasted heat of a regenerative gas turbine cycle, a heat exchanger is utilized for heating applications, a Kalina cycle is run for generating some additional power, and an ejector refrigeration cycle is used for producing some cold. The problem is firstly modeled through developing a precise code in Engineering Equation Solver program and then optimal conditions are sought by coupling the outputs of modeling procedure with Artificial Neural Network, and Non-dominated Sorting Genetic Algorithm II approaches. Three new functions of integrated weighted efficiency, exergoeconomic criterion, and exergoenvironmental criterion are defined as the system's evaluation criteria. From a robust parametric study, it is demonstrated that the system's evaluation criteria have the highest and lowest sensitivity on the variation of pressure ratio of compressor and pinch-point temperature difference of heat exchanger 2, respectively. From the optimisation procedure, the optimum values of the system's primary energy ratio, exergetic efficiency, exergoeconomic criterion, and exergoenvironmental criterion are 76.9%, 30.8%, 58.4 $/GJ, and 42.7 kg/GJ, respectively. At these conditions, the capacity of the TDES is 1025.9 kW, 1642.3 kW, and 304.9 kW with the associated cost of production of 149.6 $/GJ, 7.8 $/GJ, and 60.1 $/GJ for power, heat, and cold, respectively.

1. Introduction

Increasing the amounts of pollutant gases from one side [1] and increasing the needs for energy carriers from the other side [2] encourage researchers to seek new technologies for more efficient and cleaner energy systems. Hybrid energy systems with the ability of producing different kinds of energies in a unique system (i.e. monolithic multi-generation systems) are known as one of these technologies [3,4]. Among these systems, combined cooling, heating, and power (CCHP) trigeneration plants have attracted much attention [5]. In a hybrid multi-generation energy system, the waste heat of a prime mover cycle is recovered for running some other equipment and bottoming power/refrigeration cycle(s) [6]. Most of such systems utilize fossil fuels as the input energy source of an internal combustion engine (ICE) or gas turbine cycle (GTC) as the prime mover.

The high temperature of the exhaust gases from a GTC has a great potential to be used in heating applications together with generating some additional power in low-temperature bottoming power cycles (such as Rankine cycle (RC), organic RC (ORC), Kalina cycle (KC), etc.)

* Corresponding authors.
E-mail addresses: amir_ebrahimi_051@yahoo.com (A. Ebrahimi-Moghadam), nabuhamdeh@kau.edu.sa (N.H. Abu-Hamdeh), ashkanalimoradi@tdtu.edu.vn (A. Alimoradi).

https://doi.org/10.1016/j.enconman.2020.113581
Received 19 August 2020; Received in revised form 17 October 2020; Accepted 19 October 2020

Nomenclature

Latin letters

A	area [m^2]
c	cost per exergy unit [$/GJ]
$\dot{C}$	cost rate [$/year]
CRF	capital recovery factor [–]
e	specific exergy [kJ/kg]
$\dot{E}$	exergy rate [kW]
$\dot{E}x_{eco}$	exergoeconomic criterion [$/GJ]
$\dot{E}x_{env}$	exergoenvironmental criterion [kg/GJ]
FA	fuel–air ratio [–]
g	gravitational acceleration [m/s^2]
h	specific enthalpy [kJ/kg]
i	interest rate [%]
IWE	integrated weighted efficiency [%]
LHV	fuel lower heating value [kJ/kg]
m	pollutants emission per unit combusted fuel [$g_{pollutant}/kg_{fuel}$]
$\dot{m}$	mass flow rate [kg/s]
M	molecular weight [kg/kmol]
n	number of moles [kmol]
N	system's expected operating years [year]
P	pressure [MPa]
PER	primary energy ratio [%]
PR_{COM}	pressure ratio of compressor
$\dot{Q}$	heat rate [kW]
s	specific entropy [kJ/(kg K)]
t_{year}	system's total operating hours during a year [h]
T	temperature [K]
V	velocity [m/s]
w_1, w_2	optimisation weight coefficients [–]
$\dot{W}$	power [kW]
X	ammonia concentration in AWM [%]
z	height [m]
Z	purchase cost of equipment [$]
$\dot{Z}$	purchase cost rate of equipment [$/year]

Greek letters

η	efficiency [%]
Φ	maintenance factor [–]
$\varnothing$	equivalence ratio [–]
$\bar{\lambda}$	molar fuel–air ratio [–]
$\Pi=P_3/P_0$	dimensionless pressure of combustor [–]
$\mathscr{T}$	combustion residence time [s]
$\Theta=T_3/T_0$	dimensionless temperature of combustor [–]
Ψ	H/C atomic ratio of fuel

Abbreviations

ANN	artificial neural network
AWM	ammonia-water mixture
CHP	combined heating and power
CCHP	combined cooling, heating, and power
GTC	gas turbine cycle
KC	Kalina cycle
LMTD	logarithmic mean temperature difference
MOP	multi objective problem
RGTC	regenerative gas turbine cycle
TDES	trigeneration district energy system
ERC	ejector refrigeration cycle

Subscripts and superscripts

0	reference conditions
1 −33	state points
B	base
c	cold
CC	combustion chamber
COM	compressor
CON	condenser
CO	carbon monoxide
CO_2	carbon dioxide
D	diffuser of ejector
EJ	Ejector
EV	expansion valve
EVA	evaporator
ex	exergetic
f	injected fuel into combustor
F	fuel (in exergetic analysis)
GT	gas turbine
h	heat
H_2O	water
HEX	heat exchanger
in	inlet
is	isentropic
M	mixing chamber of ejector
MF	mixed flow
MIX	mixer (in KC)
N	nozzle of ejector
N_2	nitrogen
net	net value
NH_3	ammonia
NOx	nitrogen oxide
O_2	oxygen
O&M	operating and maintenance
out	outlet
p	power
P	product (in exergetic analysis)
PF	primary flow
PP	pinch point
PU	Pump
PZ	primary zone of combustor
RG	regenerator
SEP	separator
SF	secondary flow
tot	total

and produce cold in refrigeration cycles (such as absorption refrigeration cycle (ARC), ejector refrigeration cycle (ERC), etc.). Furthermore, low operational costs and pollutant emissions of the GTCs make them be a widely-used system for generating power [7]. Du et al. [8] used two new operation strategies for a high-temperature KC which was utilized as the bottoming cycle of a regenerative GTC (RGTC). The new operation strategies were modified sliding pressure operation (MSPO) and novel MSPO (NMSPO). They compared the results of these two new strategies with the SPO strategy and concluded that the NMSPO produces more net power, while the MSPO results in higher thermal efficiency of the KC. Gholizadeh et al. [9] proposed a new power generation system based on the combination of a biogas-fired RGTC with a modified ORC. They prepared a comprehensive energy, exergy, and exergoeconomic parametric study for evaluating their proposal. The analysis resulted in an energy efficiency of 41.8%, exergetic efficiency of 38.9%, and total product costs of 17.2 $/GJ. Singh [10] recovered the waste heat of a

Table 1
Some of the studies around hybrid energy systems based on heat recovery from GTC.

Reference	System	Analysis						Optimisation
		Energy	Exergy	Environmental	Economic	Exergoenvironmental	Exergoeconomic	
[25]	CCP	✓	✓	–	✓	–	–	✓
[26]	CCP	✓	✓	–	–	–	–	–
[27]	CHP	✓	–	–	✓	–	–	✓
[28]	CHP	✓	✓	✓	–	✓	✓	✓
[29]	CHP	✓	✓	✓	✓	–	–	–
[30]	CHP	✓	✓	✓	–	–	✓	✓
[31]	CHP	✓	✓	–	–	✓	✓	–
[32]	CCHP	✓	✓	–	–	–	✓	✓
[33]	CCHP	✓	✓	✓	–	–	✓	–
[34]	CCHP	✓	✓	✓	–	✓	✓	✓
[35]	CCHP	✓	✓	✓	✓	–	–	✓
[36]	CCHP	✓	✓	✓	✓	–	–	✓
[37]	CCHP	✓	✓	✓	–	–	✓	–

GTC-RC hybrid system for running an NH_3/H_2O ARC. He did this work for reducing the temperature of inlet air into the compressor of GTC and reported 1.2% and 1.1% improvement of the energetic and exergetic efficiencies by applying that. Cao et al. [11] developed a hybrid power generation system in which the waste heat of the GTC was recovered to use as the heat source of an ORC. They investigated the effects of different working fluids for the ORC (as bottoming cycle) and concluded that the best performance is obtained with toluene among the investigated working fluids. Wang and Dai [12] evaluated two different bottoming cycles for recovering the waste heat from a recompression supercritical CO_2 Brayton cycle (sCO_2). The bottoming cycles were transcritical CO_2 cycle (tCO_2) and ORC. They applied exergoeconomic analysis and found out that the total unit cost of electricity production of sCO_2/ORC is slightly lower than that of the sCO_2/tCO_2. Zare and Mahmoudi [13] compared the technical performance of utilizing ORC and KC as the bottoming cycle of Gas Turbine-Modular Helium Reactor (GT-MHR). At their investigated operational conditions, the results showed that the energetic efficiencies of the GT-MHR/ORC and GT-MHR/KC are respectively 11.3% and 10.3% higher than that of basic GT-MHR.

Gholizadeh et al. [14] developed a novel CCP (combined cooling and power) cogeneration system with the ability of producing cold and power simultaneously. The configuration was composed of a biogas-fired RGTC and a bi-evaporator refrigeration system. After developing the exergoeconomic model of the proposed system, they used Genetic Algorithm (GA) optimisation approach and reached the thermal efficiency, exergetic efficiency, and system costs per unit products of 62.69%, 38.75%, and 7.75 $/GJ, respectively. Xia et al. [15] combined a closed CO_2 Brayton cycle, an ORC, and an ERC for producing cold and power in a monolithic system. They considered exergoeconomic function for optimising their system through a single-objective GA optimisation. At the optimal conditions, the system cost per unit of exergy product was obtained as 63.53 $/MWh. Ebrahimi-Moghadam et al. [16] designed a combined heating and power (CHP) plant for natural gas preheating at city gate stations (CGS) instead of conventional water-bath heaters. They applied a comprehensive 4E (energy, exergy, environmental, and economic) parametric study and optimisation for their proposal. In another work, Ebrahimi-Moghadam et al. [17] also evaluated their proposal for satisfying the energy uses of a residential complex. Shokouhi Tabrizi et al. [18] used the wasted heat of a solar recompression RGTC for producing some heat to satisfy the heating uses of a natural gas CGS located in Birjand city, Iran. The outputs were 2.86 MW of electricity and payback period of 4 years for their proposal. Kim et al. [19] established a machine learning method for optimising a CHP plant. Their investigated system was based on a GTC, a steam turbine cycle, and a boiler. Also, a compressed air energy storage was considered. Based on the outputs of their new optimisation approach, the minimum thermal load of their CHP plant was 8.9 MW_{th}. Wang et al. [20] proposed two control methods for improving the performance of a CCHP system which consisted of a GTC, an ARC, and some heat exchangers. The first controlling strategy was reducing the inlet temperature of the GT, and the second one was throttling the entrance air of the compressor. Comparing the results of these two strategies, it was shown that the former is more efficient for reducing fuel consumption (by 7.53% compared to the latter). Moghimi et al. [21] examined the thermo-environmental performance of a multi-generation system made up of an RGTC, an ERC, and a water desalination unit. Their system could simultaneously produce a cold, heat, power, and freshwater of 2.03 MW, 1.1 MW, 30 MW, and 85.6 kg/s, respectively. Ebrahimi and Majidi [22] introduced a new CCHP plant and applied energetic, exergetic, and environmental principles for evaluating their system. The system was composed of a RGTC with double-stage compressor, some heat exchangers, and an ARC. Their results illustrated that the energetic and exergetic efficiencies were respectively 56% and 69% at the optimal conditions. Also, their system showed 87%, 17%, and 13% reduction of CO, CO_2, and NOx, in comparison to the conventional systems. In another work, Ebrahimi and Ahookhosh [23] developed a comprehensive thermodynamic model of a micro-scale hybrid CCHP system which was integrated from a RGTC, ORC, and ERC. Xu et al. [24] established energetic and exergetic analyses for evaluating a supercritical CO_2 CCHP system. Their findings revealed that increasing the inlet temperature of turbine leads to a significant increment in turbine's power generation and exergetic efficiency.

For having a deeper review of the previously published works in the field, some of the important ones of these studies have been categorized in Table 1.

Based on Table 1 and taking into account other relevant previously published works, it can be seen that there is still needs for more research on the exergoeconomic and exergoenvironmental models of novel trigeneration district energy systems (TDESs) with GTC mover. Furthermore, most of the researches in the field have considered simplifying assumption which causes the results to be far from the real conditions. To fulfill this gap in the literature, the objectives of the present work are focused on the design and multi-objective optimisation of a novel TDES for simultaneous production of cold, heat, and power. The novelties and contributions of this work to the state-of-the-art can be expressed as:

- ***System configuration*:**

Reviewing available literature in the field shows that no such reliable work has been conducted around a TDES based on the combination of RGTC, KC, and ERC.

- ***Methodology*:**

In the present study, a comprehensive exergoeconomic and exergoenvironmental model of the designed TDES has been developed.

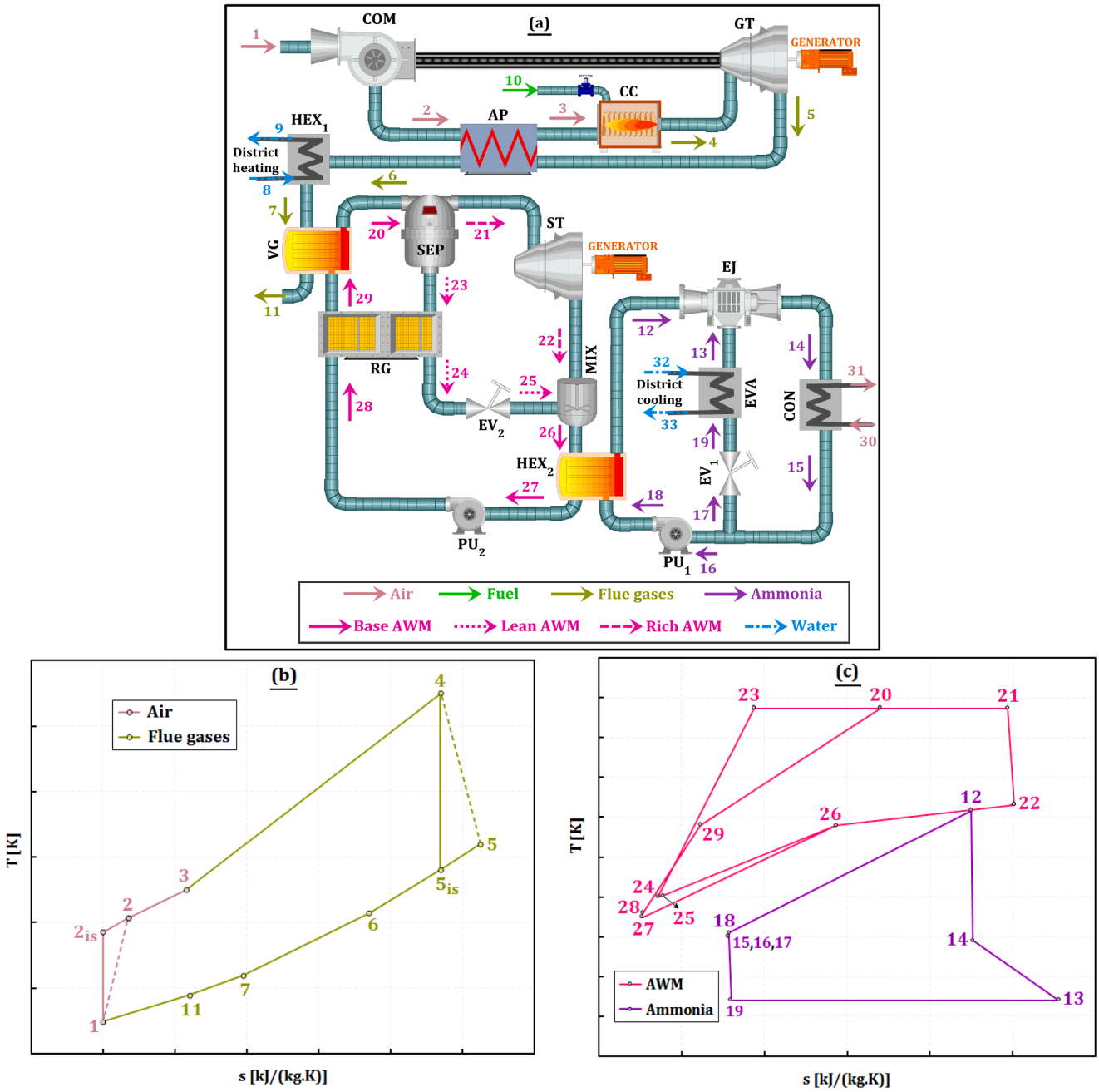

Fig. 1. (a) Schematic of the investigated TDES featuring combination of the KC and ERC for waste heat recovery from a RGTC with a heat exchanger, (b) *T-s* diagram for the RGTC, (c) *T-s* diagram for the combination of the KC and ERC.

Rational assumptions are considered for modeling the combustion reaction, and all of the important greenhouse and pollutant gases (CO_2, CO, NOx) are involved in the environmental analysis. Also, all of the effective financial indices are applied in economic evaluations. Furthermore, a comprehensive parametric sensitivity analysis is presented for studying the effects of all important parameters of the TDES on the performance criteria.

Another novelty of this work is in the solution method of the problem in which all the flow rates of the working fluids at any single points of the cycle have been given accurately as the outputs of the solutions while in the majority of works on hybrid energy systems for the sake of simplification, the flow rates of working fluids are given to the solving algorithm as the inputs. It means that the system's size is determined based on its operational conditions. Hence, the iterative approach should be applied for calculating the thermodynamic characteristics of state points.

- ***Optimisation*:**

A powerful computational code is developed for optimising the TDES. The optimisation is carried out through the combination of an artificial neural network (ANN) and non-dominated sorting GA II (NSGA-II) optimisation method. Three new criteria of integrated weighted efficiency (IWE), exergoenvironmental function ($\dot{E}x_{env}$), and exergoeconomic function ($\dot{E}x_{eco}$) are defined as the optimisation functions.

2. System configuration and operation strategy

The sketch of the investigated novel TDES in the present works is

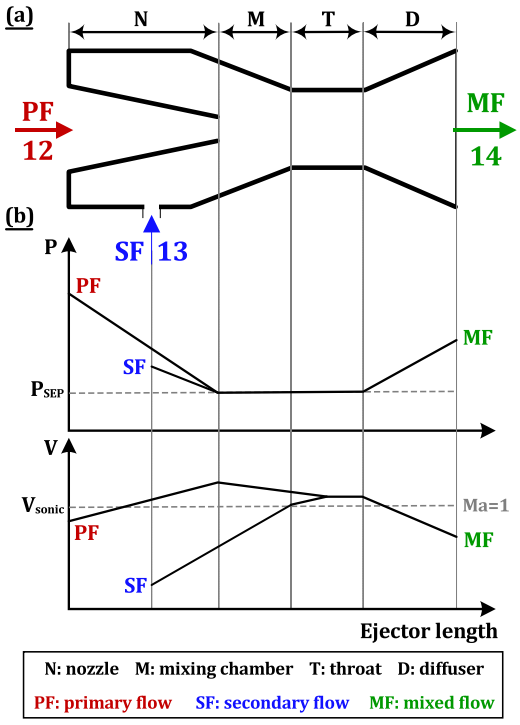

Fig. 2. (a) Schematic of the EJ, (b) pressure and velocity profile along the EJ.

depicted in Fig. 1a. The TDES comprises three sub-cycles (including an RGTC, a KC, and an ERC) with a heat exchanger which is used for heat production (HEX_1). Also, the *T-s* diagrams for each of the sub-cycles are plotted in Figs. 1b and 11c.

The RGTC acts as the mover cycle of the system. In this cycle, air with the atmospheric conditions (state 1) is compressed to a higher pressure after passing through the COM (state 2). For having a more efficient combustion reaction, the compressed air gains some heat (state 3) from the flue gases exiting from the GT (state 5) and then is guided into the CC where the combustion reaction occurs. After combustion reaction, the hot outlet gases from the CC enter the GT (state 4) and some power is produced within the process inside the GT. Continuing along the path, the heat of the hot exhaust gases is recovered for use in different purposes: preheating the air flow entering the CC (state 5), satisfying the required heat of the HEX_1 for heating applications (state 6), and satisfying the required heat for running the KC (state 7). In the VG, the base two-phase NH_3/H_2O mixture (state 29) is heated by the exhaust gases of the RGTC and then is guided into the SEP, where it is separated into the rich and lean AWMs (states 21 and 23) which respectively have higher and lower NH_3 concentrations compared to the base AWM. The rich AWM enters into the ST and is expanded (state 22) and some power is generated. The lean AWM firstly passes through RG_2 and losses some heat (state 24) and then its pressure is dropped after passing through EV_2 (state 25). Finally, these two solutions are mixed in the MIX (state 26) and then the basic two-phase AWM is fed into the HEX_2 for satisfying the required heat of running ERC. In the ERC, the EJ acts as the most important component and it has two input flow streams including the PF (i.e. state 12) and SF (i.e. state 13). These two streams are related together with the parameter of mass entrainment ratio (see Appendix A for more information). The duty of the EJ is to convert the mechanical energy of the PF (i.e. pressure) to kinetic energy (i.e. velocity). As depicted in Fig. 2, the EJ itself is composed of four main sub-components: nozzle, mixing chamber, throat, and diffuser. Hence, the modeling of the EJ is more complicated than the other system components. The EJ increases the velocity of the SF to a supersonic velocity by means of reducing the pressure of PF. So that, the PF is guided into the nozzle and is expanded within it while the pressure is significantly reduced. This pressure reduction process leads to a suction which makes the SF to enter the EJ. Then, these two streams are mixed at a constant pressure. Afterward, the MF enters the diffuser where its pressure is recovered.

3. Formulation of model

This section pays to formulate the problem under investigation. The formulation includes exergoeconomic and exergoenvironmental models. A detailed strong mathematical formulation related to each of these two analyses is presented in the following sub-sections.

3.1. Exergoeconomic model

The exergoeconomic analysis is known as a powerful approach that provides useful information about costs of productions in energy systems. This is based on the combination of the exergetic and economic analyses. The usefulness of the exergoeconomic analysis is behind in separate calculation of the cost of each energy carrier generated in multi-generation energy systems. Before developing the exergoeconomic model, the conventional energetic and exergetic analyses should be sought. Based on the system under investigation, the required equations for preparing the energetic and exergetic analyses are including mass conservation, ammonia concentration conservation, momentum conservation, energy conservation, and exergy destruction rate. The general format of the mentioned equations for steady-state condition are respectively written as follows [38–40]:

$$\sum_{\text{in}} \dot{m}_{\text{in},k} - \sum_{\text{out}} \dot{m}_{\text{out},k} = 0 \tag{1}$$

$$\sum_{\text{in}} (\dot{m}X)_{\text{in},k} - \sum_{\text{out}} (\dot{m}X)_{\text{out},k} = 0 \tag{2}$$

$$\sum_{\text{in}} (\dot{m}V)_{\text{in},k} - \sum_{\text{out}} (\dot{m}V)_{\text{out},k} = 0 \tag{3}$$

$$\left(\sum_{\text{in}} \left[\dot{m}\left(h + \frac{V^2}{2} + gz\right)\right]_{\text{in},k}\right) - \left(\sum_{\text{out}} \left[\dot{m}\left(h + \frac{V^2}{2} + gz\right)\right]_{\text{out},k}\right) + \sum \dot{Q}_k - \sum \dot{W}_k = 0 \tag{4}$$

$$\left(\sum_{\text{in}} \dot{E}_{\text{in},k}\right) - \left(\sum_{\text{out}} \dot{E}_{\text{out},k}\right) + \sum \dot{E}_{Q,k} - \sum \dot{E}_{W,k} = \dot{E}_{D,k} = \dot{E}_{F,k} - \dot{E}_{P,k} \tag{5}$$

In the above equations, the parameters $\dot{m}$, X, V, h, g, z, $\dot{Q}$, $\dot{W}$, and e denotes the mass flow rate, ammonia mass concentration in the AWM, velocity, specific enthalpy, gravitational acceleration, height, rate of heat transfer, power, and specific exergy, respectively. The terms $\dot{E}_D$, $\dot{E}_F$, $\dot{E}_P$, $\dot{E}_Q$, and $\dot{E}_W$ respectively represent the rates of exergy destruction, fuel exergy, product exergy, exergy due to the heat transfer, and exergy due

Table 2
Sumarrize of the exergoeconomic formulation of the TDES.

Component	Exergoeconomic balance	Auxiliary exergoeconomic equation
COM	$\dot{C}_2 = \dot{C}_1 + \dot{C}_{W,\mathrm{COM}} + \dot{Z}_{\mathrm{COM}}$	$c_{W,\mathrm{COMP}} = c_{W,\mathrm{GT}} c_1 = 0$
AP	$\dot{C}_3 + \dot{C}_6 = \dot{C}_2 + \dot{C}_5 + \dot{Z}_{\mathrm{AP}}$	$c_5 = c_6$
CC	$\dot{C}_4 = \dot{C}_3 + \dot{C}_{10} + \dot{Z}_{\mathrm{CC}}$	$\dot{C}_{10} = \dot{C}_f = \left(C_f \times \dot{m}_{10} \times \mathrm{LHV}\right) \times 3600 \times t_{\mathrm{year}}$
GT	$\dot{C}_5 + \dot{C}_{W,\mathrm{GT}} = \dot{C}_4 + \dot{Z}_{\mathrm{GT}}$	$c_5 = c_4$
HEX_1	$\dot{C}_7 + \dot{C}_9 = \dot{C}_6 + \dot{C}_8 + \dot{Z}_{\mathrm{HEX_1}}$	$c_7 = c_6 c_8 = 0$
EJ	$\dot{C}_{14} = \dot{C}_{12} + \dot{C}_{13} + \dot{Z}_{\mathrm{EJ}}$	–
EVA	$\dot{C}_{13} + \dot{C}_{33} = \dot{C}_{19} + \dot{C}_{32} + \dot{Z}_{\mathrm{EVA}}$	$c_{13} = c_{19} c_{32} = 0$
CON	$\dot{C}_{15} + \dot{C}_{31} = \dot{C}_{14} + \dot{C}_{30} + \dot{Z}_{\mathrm{CON}}$	$c_{15} = c_{14} c_{30} = 0$
EV_1	$\dot{C}_{19} = \dot{C}_{17} + \dot{Z}_{\mathrm{EV_1}}$	–
PU_1	$\dot{C}_{18} = \dot{C}_{16} + \dot{C}_{W,\mathrm{PU_1}} + \dot{Z}_{\mathrm{PU_1}}$	$c_{W,\mathrm{PU_1}} = c_{W,\mathrm{ST}}$
VG	$\dot{C}_{11} + \dot{C}_{20} = \dot{C}_7 + \dot{C}_{29} + \dot{Z}_{\mathrm{VG}}$	$c_{11} = c_7$
SEP	$\dot{C}_{21} + \dot{C}_{23} = \dot{C}_{20} + \dot{Z}_{\mathrm{SEP}}$	$\frac{\dot{C}_{21} - \dot{C}_{20}}{\dot{E}_{21} - \dot{E}_{20}} = \frac{\dot{C}_{23} - \dot{C}_{20}}{\dot{E}_{23} - \dot{E}_{20}}$ $c_{24} = c_{23}$
RG	$\dot{C}_{24} + \dot{C}_{29} = \dot{C}_{23} + \dot{C}_{28} + \dot{Z}_{\mathrm{RG}}$	
EV_2	$\dot{C}_{25} = \dot{C}_{24} + \dot{Z}_{\mathrm{EV_2}}$	–
MIX	$\dot{C}_{26} = \dot{C}_{22} + \dot{C}_{25} + \dot{Z}_{\mathrm{MIX}}$	–
ST	$\dot{C}_{22} + \dot{C}_{W,\mathrm{ST}} = \dot{C}_{21} + \dot{Z}_{\mathrm{ST}}$	$c_{22} = c_{21}$
HEX_2	$\dot{C}_{27} + \dot{C}_{12} = \dot{C}_{26} + \dot{C}_{18} + \dot{Z}_{\mathrm{HEX_2}}$	$c_{27} = c_{26}$
PU_2	$\dot{C}_{28} = \dot{C}_{27} + \dot{C}_{W,\mathrm{PU_2}} + \dot{Z}_{\mathrm{PU_2}}$	$c_{W,\mathrm{PU_2}} = c_{W,\mathrm{ST}}$
Division point	$\dot{C}_{15} = \dot{C}_{16} + \dot{C}_{17}$	$c_{16} = c_{17}$

to the generated power. It is worth to mention that the exergy destruction can be expressed based on the fuel and product exergy concepts (details of the formulation are presented in Appendix A). These two concepts are respectively referred to the supplied and generated exergies. Also, the indices of 'in', 'out', and '*k*' in the above equations refer to the inlet streams, outlet streams, and *k*th component in the system, respectively.

A comprehensive energetic and exergetic modeling is done and the final simplified format of the related governing equations are presented in Appendix A. Also, as two important criteria, the primary energy ratio (PER) and exergetic efficiency (η_{ex}) of the proposed TDES are respectively defined as the following equations:

$$\mathrm{PER} = \frac{\dot{Q}_c + \dot{Q}_h + \widehat{\dot{W}_{net}}}{\dot{Q}_{\mathrm{in}}} = \frac{\dot{Q}_c + \dot{Q}_h + \left(\widehat{\dot{\mathrm{W}}_{\mathrm{GT}} - \dot{\mathrm{W}}_{\mathrm{COM}} + \dot{\mathrm{W}}_{\mathrm{ST}} - \dot{\mathrm{W}}_{\mathrm{PU_1}} - \dot{\mathrm{W}}_{\mathrm{PU_2}}}\right)}{\dot{m}_{10} \times \mathrm{LHV}} \tag{6}$$

$$\eta_{\mathrm{ex}} = \frac{\dot{E}_c + \dot{E}_h + \dot{E}_p}{\dot{E}_{\mathrm{in}}} = \frac{\left(\dot{E}_{33} - \dot{E}_{32}\right) + \left(\dot{E}_9 - \dot{E}_8\right) + \dot{W}_{\mathrm{net}}}{\dot{E}_1 + \dot{E}_{10}} \tag{7}$$

where, $\dot{Q}_c$ and $\dot{Q}_h$, $\dot{W}_{\mathrm{net}}$, and $\dot{Q}_{\mathrm{in}}$ are the rates of produced cold and heat, net produced power, and input heating rate of the proposed TDES; also, $\dot{E}_c$, $\dot{E}_h$, $\dot{E}_p$, and $\dot{E}_{\mathrm{in}}$ are exergy rates due to the produced cold, heat, and power, and system's input exergy rate.

The exergoeconomic analysis includes the cost balance equation which is expressed as Eq. (8) for *k*th component. Based on this equation, it can be stated that the cost associated with the outlet exergy streams equals the cost of inlet exergy streams plus the system's costs and other costs [41].

$$\left(\sum_{\mathrm{in}} \dot{C}_{\mathrm{in},k}\right) - \left(\sum_{\mathrm{out}} \dot{C}_{\mathrm{out},k}\right) + \left(\sum \dot{C}_{Q,k}\right) - \left(\sum \dot{C}_{W,k}\right) + \dot{Z}_k = 0 \tag{8}$$

where, $\dot{C}$ indicates the cost rate associated with an exergy stream and $\dot{Z}$ denotes total cost rate for system components which is obtained through the summation of capital investment (CI) and operating & maintenance (OM) costs. These two definitions are expressed as Eqs. (9) and (10) [42].

$$\dot{C}_k = c_k \dot{E}_k = c_k (\dot{m}e)_k \tag{9}$$

$$\dot{Z}_k = \dot{Z}_k^{\mathrm{CI}} + \dot{Z}_k^{\mathrm{OM}} = Z_k \times \mathrm{CRF} \times \Phi \tag{10}$$

where, c and Z_k respectively signify the costs per unit of exergy and capital investment cost (or purchase cost) of the *k*-th component. It is worth mentioning that reliable cost functions are used for accurate calculation of the purchase cost of the system components based on the system's operating conditions (related information are presented in Appendix B). Also, Φ is maintenance factor which is considered to be 1.06 and CRF is the capital recovery factor which is defined as the following equation [43]:

$$\mathrm{CRF} = i \times \left[\frac{(1+i)^N}{(1+i)^N - 1}\right] \tag{11}$$

where, i and N represent the interest rate and system's expected operating years, respectively.

Combining the cost balance equation and exergy rules results in the exergoeconomic equation as follows:

$$\left(\sum_{\text{in}}\left[c_{\text{in}}\dot{E}_{\text{in}}\right]_k\right)-\left(\sum_{\text{out}}\left[c_{\text{out}}\dot{E}_{\text{out}}\right]_k\right)+\left(\sum\left[c_Q\dot{E}_Q\right]_k\right)-\left(\sum\left[c_W\dot{E}_W\right]_k\right)+\dot{Z}_k=0 \tag{12}$$

The notable point to solve the exergoeconomic equation for each system component is that the auxiliary exergoeconomic equation(s) is (are) needed for some components that include more than one exiting exergy stream. The final format of the cost balance and required auxiliary equations for all the system components are presented in Table 2.

The costs of the produced cold, heat, and net power can respectively be calculated using the following formulas:

$$c_c=\frac{\dot{C}_{33}}{\dot{E}_{33}} \tag{13}$$

$$c_h=\frac{\dot{C}_9}{\dot{E}_9} \tag{14}$$

$$c_p=\frac{\dot{C}_{W,\text{net}}}{\dot{W}_{\text{net}}}=\frac{\dot{C}_{W,\text{GT}}-\dot{C}_{W,\text{COM}}+\dot{C}_{W,\text{ST}}-\dot{C}_{W,\text{PU}_1}-\dot{C}_{W,\text{PU}_2}}{\dot{W}_{\text{GT}}-\dot{W}_{\text{COM}}+\dot{W}_{\text{ST}}-\dot{W}_{\text{PU}_1}-\dot{W}_{\text{PU}_2}} \tag{15}$$

Finally, the exergoeconomic criterion is developed as the following equation:

$$\dot{\text{Ex}}_{\text{eco}}=\frac{\dot{C}_{W,\text{net}}+\dot{C}_9+\dot{C}_{33}}{\dot{W}_{\text{net}}+\dot{E}_9+\dot{E}_{33}} \tag{16}$$

3.2. Exergoenvironmental model

Environmental assessment of the multi-generation energy systems is one of the important steps in the evaluation of the system's performance. The impact of the system on the environment becomes more valuable when evaluated based on the system products. Here, a powerful exergoenvironmental model is developed which is based on the combination of the conventional exergy and environmental analyses.

As the first step, the emission rate of harmful gases should be determined before the exergoenvironmental analysis. To have a precise environmental model, in the present investigation, the combustion reaction of the fuel is solved and then the amount of the all pollutant and greenhouse gases are calculated. The combustion reaction of any desired hydrocarbon can be written as Eq. (17) [44]. Based on this equation, the exergoenvironmental analysis in the present work includes the effect of pollutant gases of carbon monoxide (CO) and nitrogen oxide (NOx) and greenhouse gas of carbon dioxide (CO_2).

$$\bar{\lambda}\text{C}_{x_1}\text{H}_{x_2}+(x_{\text{O}_2}\text{O}_2+x_{\text{N}_2}\text{N}_2+x_{\text{H}_2\text{O}}\text{H}_2\text{O}+x_{\text{CO}_2}\text{CO}_2)\rightarrow y_{\text{CO}_2}\text{CO}_2+y_{\text{N}_2}\text{N}_2+\text{y}_{\text{O}_2}\text{O}_2+y_{\text{H}_2\text{O}}\text{H}_2\text{O}+y_{\text{NO}}\text{NO}+y_{\text{CO}}\text{CO} \tag{17}$$

in which, $\bar{\lambda}$ is molar fuel–air ratio which is defined as Eq. (18). Also, after the atomic balance of the combustion reaction, the details of molar analysis can be written as Eq. (19). It should be noted that the mole fraction of the air entering into the system includes 20.59% O_2, 77.48% N_2, 1.90% H2O (g), and 0.03% CO_2. Also, methane (CH_4) is assumed as the fuel injected into the CC.

$$\bar{\lambda}=\frac{n_{10}}{n_1} \tag{18}$$

$$y_{\text{CO}_2}=\bar{\lambda}x_1+x_{\text{CO}_2}-y_{\text{CO}}$$

$$y_{\text{N}_2}=x_{\text{N}_2}-y_{\text{NO}}$$

$$y_{\text{H}_2\text{O}}=x_{\text{H}_2\text{O}}+\frac{\bar{\lambda}x_2}{2}$$

$$y_{\text{O}_2}=x_{\text{O}_2}-\bar{\lambda}x_1-\frac{\bar{\lambda}x_2}{4}-\frac{y_{\text{NO}}}{2}-\frac{y_{\text{CO}}}{2} \tag{19}$$

Accurate correlations (which are developed based on the real experiments) are used for estimating the amount of these gases as expressed in Eqs. (20) and (21) [45].

$$m_{\text{CO}}=\frac{0.179\times10^9\exp(7800/T_{\text{PZ}})}{P_3^2\mathscr{T}(\Delta P_{\text{CC}}/P_3)^{0.5}} \tag{20}$$

$$m_{\text{NOx}}=\frac{0.15\times10^{16}\mathscr{T}^{0.5}\exp(-71100/T_{\text{PZ}})}{P_3^{0.05}(\Delta P_{\text{CC}}/P_3)^{0.5}} \tag{21}$$

in which, m_{CO} and m_{NOx} are grams of the CO and NOx which are released per kilogram of the fuel which is burned in the CC (i.e. $g_{\text{pollutant}}/kg_{\text{fuel}}$). Hence, Eq. (22) should be used for determining the mass flow rate of these gases (i.e. $kg_{\text{pollutant}}/s$). In the above correlations, the residence time is generally assumed to be $\mathscr{T}=2$ ms and the parameter of T_{PZ} represents the temperature of the CC's primary zone which is calculated using Eq. (23) [16].

$$\dot{m}_{\text{NOx}}=m_{\text{CO}}\times10^{-3}\times\dot{m}_{10},\dot{m}_{\text{NOx}}=m_{\text{CO}}\times10^{-3}\times\dot{m}_{10} \tag{22}$$

$$T_{\text{PZ}}=\mathscr{C}\delta^{x}\exp\left(\vartheta(\delta+\varepsilon)^2\right)\Pi^{x^*}\Theta^{y^*}\Psi^{z^*} \tag{23}$$

Details of the required parameters in Eq. (23) are presented in Appendix C.

Finally, the exergoenvironmental criterion is developed as the following equation:

$$\dot{\text{Ex}}_{\text{env}}=\frac{\dot{m}_{\text{CO}}+\dot{m}_{\text{NOx}}+\dot{m}_{\text{CO}_2}}{\dot{W}_{\text{net}}+\dot{E}_9+\dot{E}_{33}} \tag{24}$$

The governing equations of the problem are solved through developing an accurate computational code in Engineering Equation Solver (EES) software. More details are presented in the next sections.

4. Optimisation procedure

As mentioned before, the governing equations are solved using EES software. For the optimisation procedure in the present study, a powerful computational code is developed in Matlab software. Hence,

Table 3
Main considered parameters of the NSGA-II optimisation procedure in the present study.

Parameter	Value
Chromosome number of each individual	6
Individuals number of the population	150
Maximum iteration number	200
Mutation probability	0.7
Crossover probability	0.3

an intermediary tool should be used for coupling the outputs of the modeling procedure from EES to be usable for the optimisation procedure in Matlab. Here, an artificial neural network (ANN) is trained to re-model the system, and then the proposed multi-objective problem (MOP) is solved by a non-dominated sorting genetic algorithm II (NSGA-II) approach in Matlab to find most preferred solutions. Finally, the Linear Programming Technique for Multidimensional Analysis of Preference (LINMAP) method is applied to select the final optimal solution. In the rest, the detailed description is given for different parts of the optimisation procedure section.

4.1. Artificial neural network

As mentioned in the previous section, an ANN is carried out as an intermediary tool for coupling the EES outputs with the optimisation procedure in Matlab. In this way, firstly, a data bank should be created through a parametric study in the EES and then the numeric data of this bank are imported to the ANN. The ANN learns the existing relationship between the inputs (i.e. the system's design parameters) and outputs (i.e. the defined evaluation criteria) based on this data bank [46].

Generally, an ANN is composed of some layers including an input layer, hidden layer(s), and an output layer. Each design parameter is related to a neuron in the input layer, and after applying a weight it is connected to the other ones in the first hidden layer. Afterward, the summation of these weighted values is affected by a transfer function to give an output. There are two types of transfer functions in any AAN: the first one is called activation function (AF) in the present study and is for hidden layers(s), and the second one is for output layer which here is called the output function (OF). Regarding a general view of the proposed ANN architecture, the proposed ANN model receives six parameters of PR_{COM}, T_{GT}, X_B, P_{VG}, $\Delta T_{PP,HEX_2}$, and T_{EVA} as inputs and gives four evaluation criteria of PER, η_{ex}, $\dot{E}x_{eco}$, and $\dot{E}x_{env}$ as the outputs of the network. For increasing the accuracy, in the present investigation, four Feed-Forward Networks are separately trained to re-model each of the system's evaluation criteria. It means that the number of neurons in the input and output layers is respectively equal to 6 and 1 neurons, for each of the four designed ANNs. The structure of all these ANNs is the same, with two hidden layers and four neurons in each of them. Moreover, Levenberg-Marquardt backpropagation is used to train the networks.

The formulation of the ANN in the present study can be written as the following equations. Based on the network architecture and considered assumptions, the log-sigmoid (logsig) and linear (purelin) functions are respectively considered for the AF and OF (Eqs. (28) and (29)) [47]. It is worth to mention that a large data bank with 32,140 data set is used as the input of the ANN, and 70%, 15%, and 15% of data are considered for training, validation, and testing, respectively.

$$\widehat{M}_j = g_{AF}\left(\sum_{t=1}^{6}\sum_{j=1}^{4} m_{j,t}\widehat{I}_t + b_{1,j}\right) \tag{25}$$

$$\widehat{N}_j = g_{AF}\left(\sum_{t=1}^{4}\sum_{j=1}^{4} n_{j,t}\widehat{M}_t + b_{2,j}\right) \tag{26}$$

$$\widehat{O}_j = g_{OF}\left(\sum_{t=1}^{4} o_t\widehat{N}_t + b_3\right) \tag{27}$$

$$AF = g(a) = \text{logsig}(a) = \frac{1}{1+e^{-a}}; [-1, 1] \tag{28}$$

$$OF = g(a) = \text{purelin}(a) = a; (-\infty, \infty) \tag{29}$$

where, the vectors $\widehat{I}$, $\widehat{M}$, $\widehat{N}$, and $\widehat{O}$ respectively refer to the system's design parameters, outputs of the first hidden layer, outputs of the second hidden layer, and system's evaluation criteria. Also, the parameters $m_{j,t}$, $n_{j,t}$, and o_t and $b_{1,j}$, $b_{2,j}$, and $b_{3,j}$ are interconnection weights and biases of different layers.

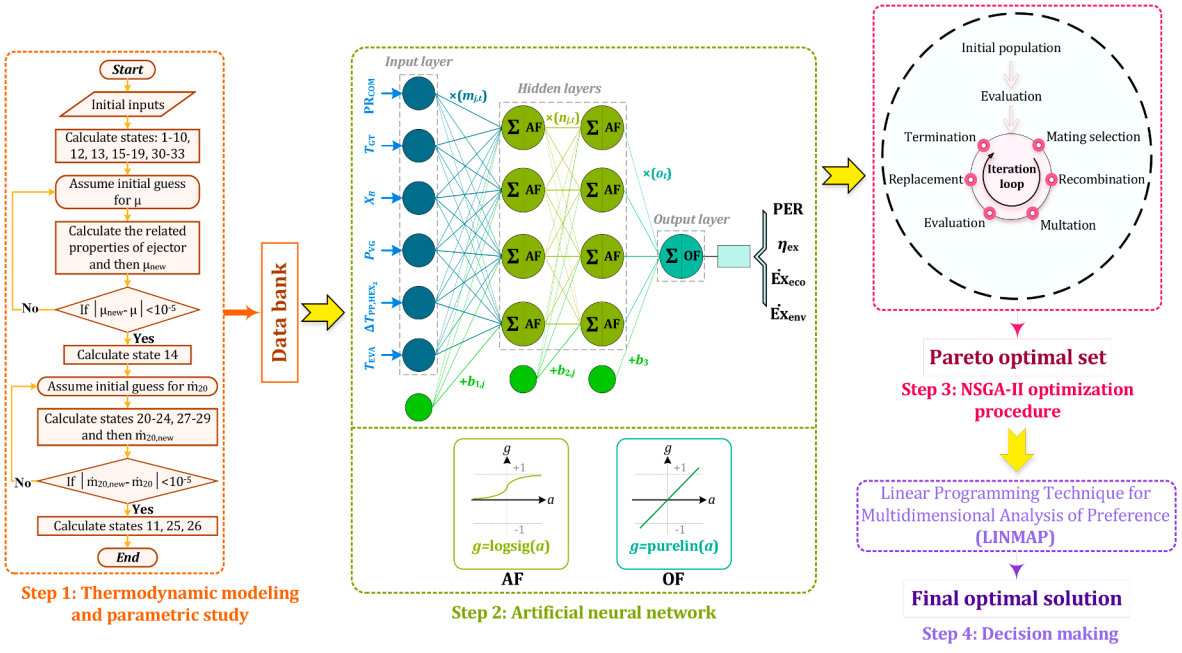

Fig. 3. Illustrative sketch of the modeling and optimisation procedures.

Table 4
Validation of the outputs of the modeling procedure for the RGTC and KC.

Cycle	Parameter	Present work	Reference works	Deviation
RGTC			Bejan et al. [55]	
	Molar fuel–air ratio	0.03053	0.0321	4.89%
	Outlet temperature of GT	995.88 K	1006.162 K	1.02%
	Energy efficiency	84.28%	n/a[a]	–
	Exergy efficiency	49.86%	50.3%	0.87%
KC			Ghaebi et al. [56]	
	Produced power	275.2 kW	286.3 kW	3.88%
	Heat rate of VG	3967 kW	3964 kW	0.07%
	Energy efficiency	6.94%	7.22%	3.88%
	Ammonia fraction in the rich AWM	0.9997	0.9997	0

[a] n/a: not available data in the reference work.

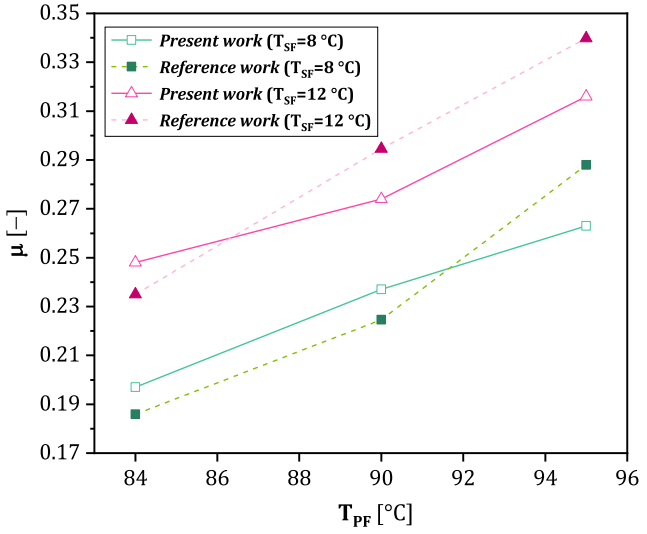

Fig. 4. Comparison of the outputs of the ERC between the present work and those of Huang et al. [57].

4.2. Proposed multi-objective problem

Due to the variety of the design parameters (i.e. inputs) and the system's evaluation criteria (i.e. objective functions), there are various interactions between conflicting objectives. In the other word, in MOPs, there are more than one objective function and the problem objective functions are in conflict with each other; i.e. trying to improve one of them in worsening the results for others. In MOP, the concept of optimality is replaced with that of efficiency or Pareto optimality [48–50]. The Pareto optimal solutions are solutions that cannot be improved in one objective, unless worsening the solution in another objective. In general, a MOP can be formulated as follows:

$$\text{Maximise or Minimise } F(x) = [f_1, f_2, \cdots, f_c]^T,\ \hat{x} = (x_1, x_2, \cdots, x_d)$$

$$\text{subject to: } H(x) = 0;$$

$$G(x) \le 0; \tag{30}$$

where, the vectors F and $\hat{x}$ respectively contain the evaluation criteria and design parameters.

From the defined evaluation criteria in the present work, PER and η_{ex} should be maximised and $\dot{E}x_{eco}$ and $\dot{E}x_{env}$ should be minimised. As PER and η_{ex} are of the same genus (both of them have the nature of the efficiency), these two criteria are converted to a new function named integrated weighted efficiency (IWE) using by weighted sum method (WSM). The WSM has been used in different studies in the field [51–53]. This function optimises the PER and η_{ex} simultaneously and leads to better results compared to energy- or exergy-alone optimisations. In the WSM, based on the desired design conditions/limitations of the problem, the weights should be selected in accordance with Eq. (32).

Table 5
The performance evaluation of the calculated networks for each evaluation criterion.

Statistical criterion	System's evaluation criterion		
	IWE	$\dot{E}x_{eco}$	$\dot{E}x_{env}$
RMSE	0.1469	0.9652	0.2942
MAE	0.0963	0.3790	0.2036
R	0.9998	0.9940	0.9997

$$\text{IWE} = w_1 \text{PER} + w_2 \eta_{ex} \tag{31}$$

$$w_1 + w_2 = 1,\ 0 \le w_1,\ w_2 \le 1 \tag{32}$$

In the present study, an equal contribution is considered for PER and η_{ex} in the optimisation procedure. Consequently, equal weights are considered for both of these two evaluation criteria (i.e. $w_1 = w_2 = 0.5$). Finally, the proposed MOP for the parameter designing of the proposed system can be formulated as follows:

$$\text{Min}_x\{F_1, F_2, F_3\}, x = [\text{PR}_{\text{COM}}, T_{\text{GT}}, X_B, P_{\text{VG}}, \Delta T_{\text{PP,HEX}_2}, T_{\text{EVA}}] \tag{33}$$

$$\begin{cases} F_1 = -\text{IWE} \\ F_2 = \dot{E}x_{eco} \\ F_3 = \dot{E}x_{env} \\ X_{LB} \le x \le X_{UB} \\ X_{LB} = [5, 1200, 0.5, 25, 5, 273] \\ X_{UB} = [15, 1400, 0.8, 35, 15, 283] \end{cases} \tag{34}$$

where, X_{LB} and X_{UB} represent the lower and upper bounds for each of the evaluation criteria.

In the present study, the non-dominated sorting genetic algorithm II (NSGA-II) approach is used which is more suitable than simple GA for MOPs. The setting specifications for the NSGA-II in the present study are listed in Table 3.

4.3. Decision-making

As the main difference between MOP and SOP (single-objective problem), there is not a single optimal solution that would simultaneously optimise all objectives in MOP. In this type of the optimisation problem, the Pareto optimal solutions are replaced with an optimal solution. Hence, a decision-making method should be used to select the most preferred solution with the best compromise between objective functions after finding Pareto optimal set. Taking into account previous works in the field [54], the LINMAP method is applied as the decision-making method of the proposed model to select the final optimal solution in this paper. The LINMAP method is performed as follows:

- For each solution, a nondimensional value should be calculated based on Eq. (35) for each objective separately.
- An unattainable ideal point ($f^*_{\text{ideal},1}, f^*_{\text{ideal},2}, f^*_{\text{ideal},3}$) should be determined considering the results obtained in the Pareto front through applying Eq. (36).
- The normalized distance d_i should be calculated by Eq. (37) for each of the Pareto front results from the ideal point.
- The solution with having the lowest normalized distance is selected as the preferred optimal solution.

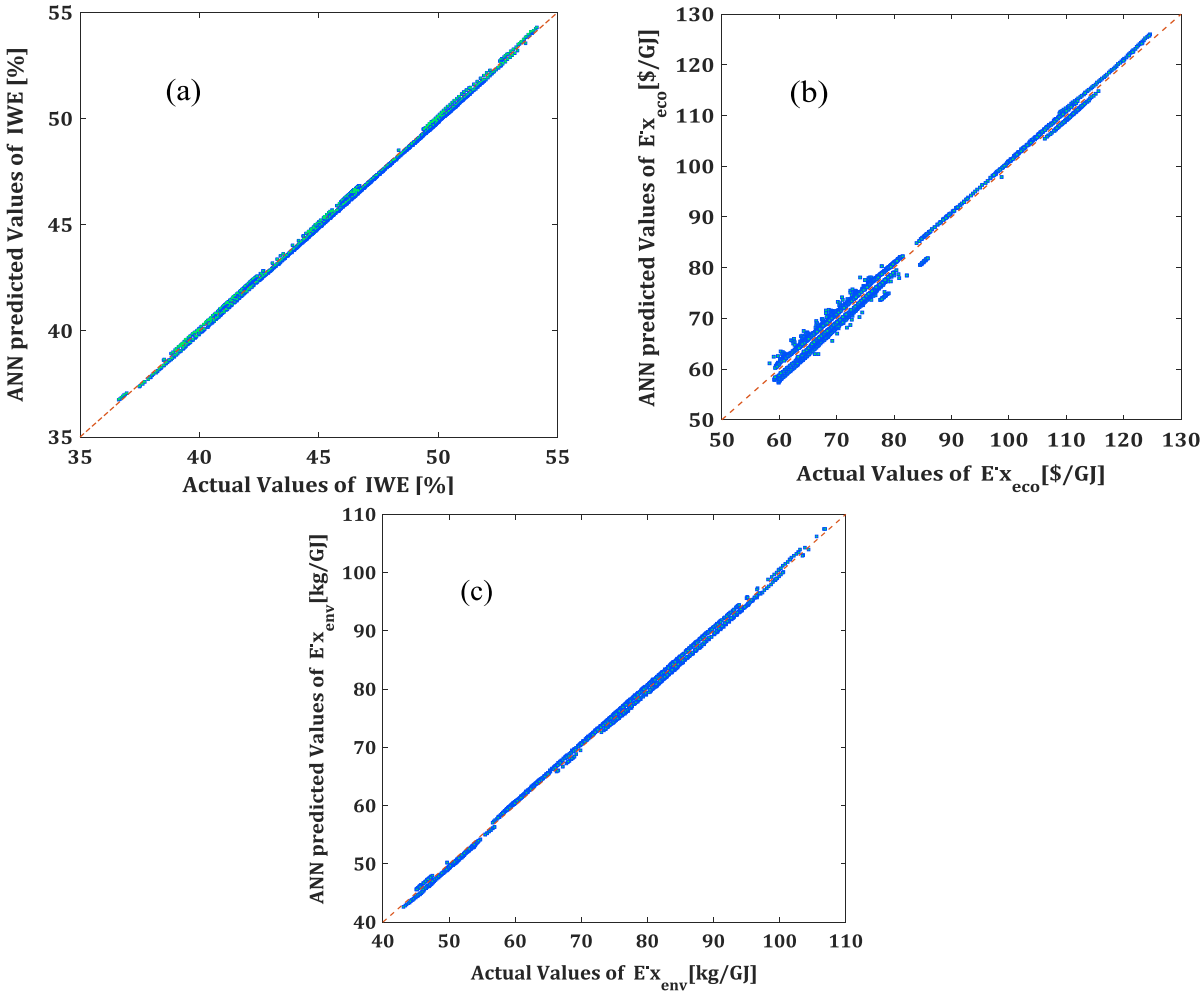

Fig. 5. Comparison of actual data generated from the proposed system and the predicted data by ANN for, (a) integrated weighted efficiency, (b) exergoeconomic criterion, (c) exergoenvironmental criterion.

$$f_{i,j}^{*}=\frac{f_{i,j}}{\sqrt{\sum_{i=1}^{N}(f_{i,j})^{2}}},\ j=1,2,3 \tag{35}$$

$$f_{\text{ideal},j}^{*}=\min_{i} f_{i,j},\ j=1,2,3 \tag{36}$$

$$d_{i}=\sqrt{\sum_{j=1}^{3} w_{j}\left(f_{i,j}^{*}-f_{\text{ideal},j}^{*}\right)^{2}} \tag{37}$$

5. Summary of the modeling procedure

A schematic diagram of the system's thermodynamic modeling and optimisation procedures is shown in Fig. 3. Since none of the sub-cycles' mass flow rates are considered as the input parameters of the problem, the thermodynamic characteristics of state points are calculated using the iterative method with enough accuracy (from the order of 10^{-5}). After system modeling, a comprehensive parametric study is done for studying the impact of the some system's design parameters on four evaluation criteria of PER, η_{ex}, $\dot{E}x_{eco}$, and $\dot{E}x_{env}$. Afterward, an accurate ANN is designed for re-modeling the problem and knowing the relation and interaction between design parameters and evaluation criteria. As the final step, the outputs of the ANN are used as the input of NSGA-II for optimising the problem.

6. Validation procedure

6.1. Validation of model

The validity of any combined energy system will be proven when the outputs related to each of its sub-systems be validated. Accordingly, in the present study, three reliable reference works are considered for validating the outputs of the RGTC [55], KC [56], and ERC [57]. The comparison of the results is presented in Table 4 and Fig. 4. Comparing the results showed that the average of the relative deviation between the present and reference works are 2.26%, 1.96%, and 6.6% for RGTC, KC, and ERC, respectively. This indicates the validity of the results of the present work compared to the considered reliable reference investigations. Also, the reason of the deviation could be found in the method of problem modeling and the difference of softwares in which the computational codes have been developed.

6.2. Validation of ANN

The ANN is used for fitting the objectives of the problem and the specific network is separately carried out for each of them. The performance of the calculated networks is evaluated using three different standard statistical criteria including the Root Mean Square Error (RMSE), the Mean Absolute Error (MAE), and the correlation coefficient (R). These statistical criteria are formulated as Eqs. (38)–(40) [58].

Table 6
The input parameters of the modeling procedure and their assumed value [55,59].

Parameter		Symbol	Value
Reference temperature/pressure		T_0/ P_0	289.15 K/0.101 MPa
Pressure ratio of COM		PR_{COM}	10
Isentropic efficiency of	COM	$\eta_{COM,is}$	86%
	GT	$\eta_{GT,is}$	86%
	ST	$\eta_{ST,is}$	90%
	PU	$\eta_{PU_1,is}$, $\eta_{PU_2,is}$	90%, 90%
Pressure drop within	AP (air side)	$\Delta P_{AP,a}$	5%
	AP (flue gases side)	$\Delta P_{AP,g}$	3%
	CC	ΔP_{CC}	5%
	HEX_1 (flue gases side)	ΔP_{HEX_1}	5%
Inlet temperature of CC		T_3	820 K
Thermal efficiency of CC		η_{CC}	98%
Fuel supply pressure		P_{10}	1.2 MPa
District heating supply/return temperature		T_9/T_8	353.15 K/313.15 K
Ammonia mass fraction in base AWM		X_B	0.6
Terminal temperature difference of VG		TTD_{VG}	15 K
Pinch point temperature difference of RG		$\Delta T_{PP,RG}$	10 K
Isentropic efficiency of EJ's nozzle		$\eta_{N,is}$	85%
Efficiency of EJ's mixing chamber		η_M	90%
Isentropic efficiency of EJ's diffuser		$\eta_{D,is}$	85%
District cooling supply/return temperature		T_{33}/ T_{32}	281.15 K/288.15 K
Fuel cost/ lower heating value		C_f/ LHV	2.5 $/GJ/50916.96 kJ/kg
System's total operating hours during a year		t_{year}	7000 h
System's expected operating years		N	20 years
Interest rate		i	8%

$$\mathrm{RMSE} = \sqrt{\frac{\sum_{i=1}^{N}(y_{t,i} - y_{f,i})^2}{N}} \tag{38}$$

$$\mathrm{MAE} = \frac{\sum_{i=1}^{N}|y_{t,i} - y_{f,i}|}{N} \tag{39}$$

$$R = \frac{\sum_{i=1}^{N}(y_{t,i} - \overline{y_t})(y_{f,i} - \overline{y_f})}{\sqrt{(y_{t,i} - \overline{y_t})^2}\sqrt{(y_{f,i} - \overline{y_f})^2}} \tag{40}$$

in which, $y_{t,i}$ and $y_{f,i}$ are target data and forecast data. Also, $\overline{y_t}$ and $\overline{y_f}$ are the mean of the each of these data.

The performance indices of the ANN are presented in Table 5. The results demonstrate that the designed ANN predicts the data accurately. Also, the comparison between the outputs of the system's modeling procedure with those predicted by the ANN for defined evaluation criteria is plotted in Fig. 5. Based on this figure, the ANN could predict the outputs more precisely, as the points in this figure get closer to the 45° line. In the other words, the closer R values to the unity indicate the lower difference between the results.

7. Results and discussion

Based on the objectives of the present work, this section is divided into three sub-sections. Firstly, the results of the base TDES is presented with input parameters as listed in Table 6. In the second sub-section, a comprehensive parametric study is sought for evaluating the impact of all the important design parameters on the defined evaluation criteria. Finally, a powerful optimisation is applied to achieve the optimal conditions of the designed TDES. It is worth to mention that a wide range of the system's investigated design parameters is considered for parametric study and optimisation: pressure ratio of the compressor ($5 \leq PR_{COM}$[–] ≤ 15), inlet temperature of the gas turbine ($1200 \leq T_{GT}$[K] ≤ 1400), mass fraction of ammonia in the basic ammonia-water mixture ($50 \leq X_B$[%] ≤ 80), pressure of the vapor generator ($2.5 \leq P_{VG}$[MPa] ≤ 3.5), pinch-point temperature difference of the heat exchanger 2 ($5 \leq \Delta T_{PP,HEX_2}$[K] ≤ 15), and temperature of the evaporator ($274 \leq T_{EVA}$[K] ≤ 283).

Table 7
Thermo-physical characteristics at state points of the TDES.

State point	T [K]	P [MPa]	h [kJ/kg]	s [kJ/(kgK)]	X [–]
1	298.15	0.101	298.57	5.70	–
2	614.11	1.013	622.16	5.77	–
3	700	0.962	713.58	5.93	–
4	1300	0.914	1396.11	6.64	–
5	840.69	0.110	867.13	6.75	–
6	629.11	0.107	638	6.44	–
7	439.53	0.101	437.68	6.09	–
8	313.15	1.200	168.56	0.57	–
9	353.15	1.200	335.84	1.07	–
10	298.15	1.200	−4649.72	10.33	–
11	378.74	0.101	379.75	5.94	–
12	373.15	6.257	1436.49	4.50	–
13	278.15	0.516	1467.38	5.56	–
14	308.15	1.351	1276.98	4.52	–
15	308.15	1.351	366.08	1.57	–
16	308.15	1.351	366.08	1.57	–
17	308.15	1.351	366.08	1.57	–
18	309.77	6.257	375.33	1.57	–
19	278.15	0.516	366.08	1.60	–
20	424.53	3	1086.36	3.40	0.6
21	424.53	3	1694.17	4.94	0.872
22	376.28	0.926	1512.74	4.99	0.872
23	424.53	3	481.9	1.88	0.3295
24	330.11	3	46.39	0.72	0.3295
25	330.48	0.926	46.39	0.73	0.3295
26	365.73	0.926	777.54	2.87	0.6
27	319.77	0.926	−15.48	0.54	0.6
28	320.11	3	−12.47	0.54	0.6
29	366	3	205.88	1.18	0.6
30	293.15	0.101	293.55	5.68	–
31	310.15	0.101	310.63	5.74	–
32	288.15	0.101	63.01	0.22	–
33	281.15	0.101	33.71	0.12	–

Table 8
The rates of the exergy destruction, cost of exergy destruction, and investment cost, for each of the TDES components.

Component	$\dot{E}_D$ [kW]	$\dot{C}_D$ [$/yr]	$\dot{Z}$ [$/y]
CC	1210.8	132,639	496.4
COM	107.1	16435.7	18898.1
GT	152.7	21645.5	7927.7
HEX_1	349	49454.2	479.3
RG_1	419.9	63,026	8285.8
ST	3.5	462.7	7351.3
VG	8.3	922.4	2076.1
SEP	0.5	92.9	8.7
RG_2	5.3	988.9	204.3
MIX	1.3	250.5	8.7
PU_2	0.1	40.6	62.6
EV_2	0.4	63.4	3.0
HEX_2	8.9	1379.7	298.0
CON	9.3	3171	894.3
EJ	29.8	14839.2	604.6
EV_1	0.7	365.2	1.5
PU_1	0.2	96.3	77.7
EVA	2.1	1047.3	865.1

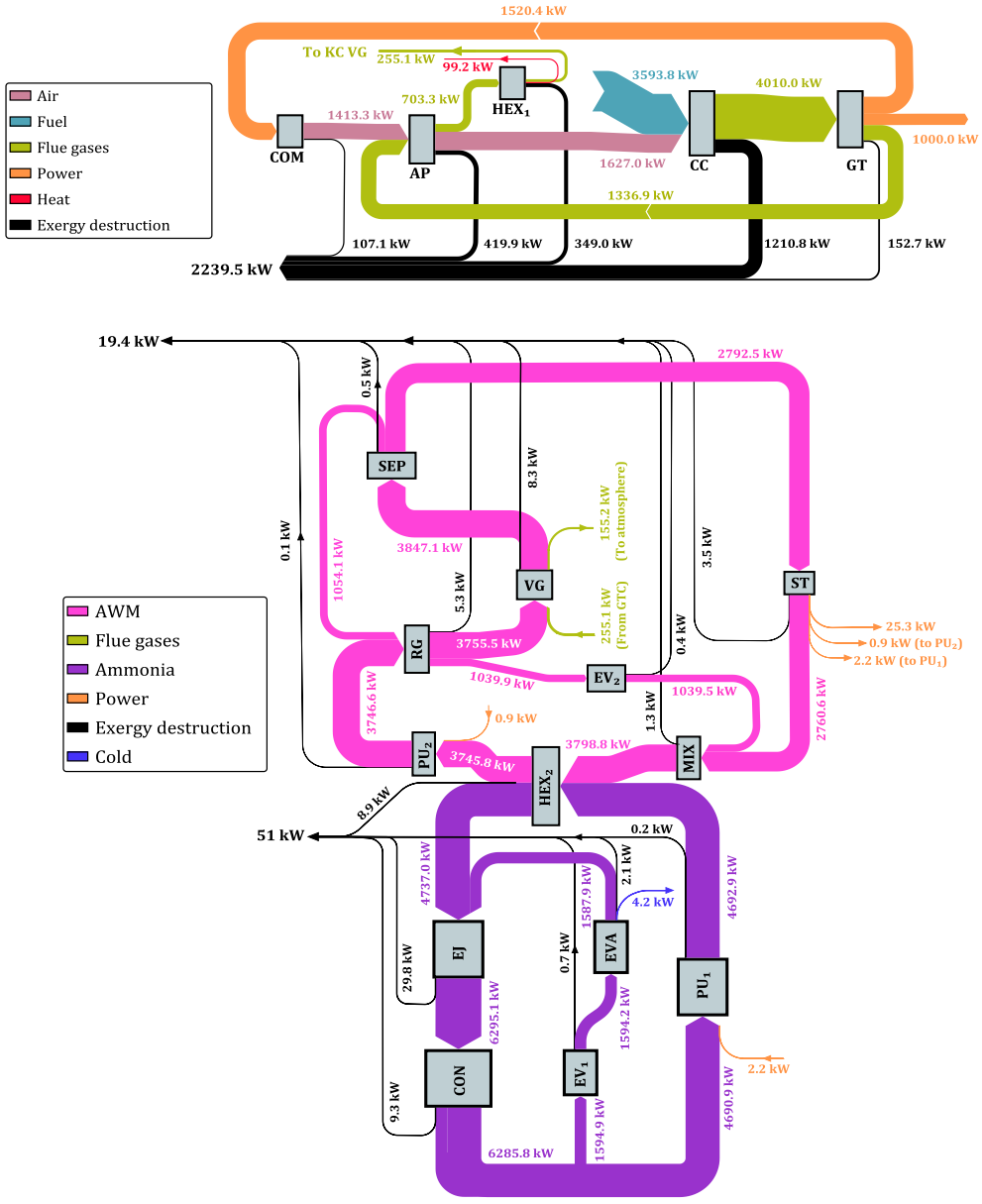

Fig. 6. Sankey exergy flow diagram of the investigated TDES.

7.1. Results of the model for the base TDES

Thermodynamic modeling is the first step before developing exergoeconomic and exergoenvironmental models. Thermodynamic modeling is started by calculating all the required thermo-physical characteristics of the state points in the system. The outputs of this step are presented in Table 7.

Taking into account Table 8, the results illustrate that the maximum and minimum values of the exergy destruction and cost of exergy destruction occur in CC (with $\dot{E}_D = 1210.8$ kW and $\dot{C}_D = 132639$ \$/y) and PU_2 (with $\dot{E}_D = 0.1$ kW and $\dot{C}_D = 40.6$ \$/y), respectively. Also, the maximum and minimum values of the rate of investment cost is related to COM (with $\dot{Z} = 18898.1$ \$/y) and EV_1 (with $\dot{Z} = 1.5$ \$/y), respectively.

Fig. 6 shows useful information about the exergy flow within the TDES. Based on this figure, 52.6%, 9.7%, 0.5%, and 1.4% of the system's total input exergy rate (i.e. 3593.8 kW) is respectively destroyed in RGTC, HEX_1, KC, and ERC. Also, the useful exergy rates of the net power, heat, and cold are 1025.25 kW, 99.2 kW, and 4.2 kW, respectively. This results in the exergetic efficiency of the TDES to be $\eta_{ex} = 31.41\%$.

The share of each sub-cycles and components of the TDES from the total cost rate is illustrated in Fig. 7. This figure reveals that 29.23% of the system's total cost rate is due to penalty of the pollutants and greenhouse gas emissions. From the enviro-economic standpoint, it can be inferred that most of the penalty costs are related to CO_2, while the impact of the CO and NOx is ignorable. Furthermore, the investment cost rate of ERC is much lower than that of the RGTC and KC. So that, only 5.65% of the total investment cost rate is related to the ERC.

Finally, the major outputs of the energetic, exergetic, exergoeconomic, and exergoenvironmental analyses are listed in Table 9. At the base conditions, the rates of the produced power, heat, and cold are respectively 1025.25 kW, 954.48 kW, and 87.72 kW, and the associate costs for producing these energies are respectively 161.01 \$/GJ, 7.67 \$/GJ, and 58.05 \$/GJ.

7.2. Results of the model for sensitivity analysis

This section discusses the outputs of the parametric study for the design parameters of the RGTC (Figs. 8 and 9) and KC and ERC

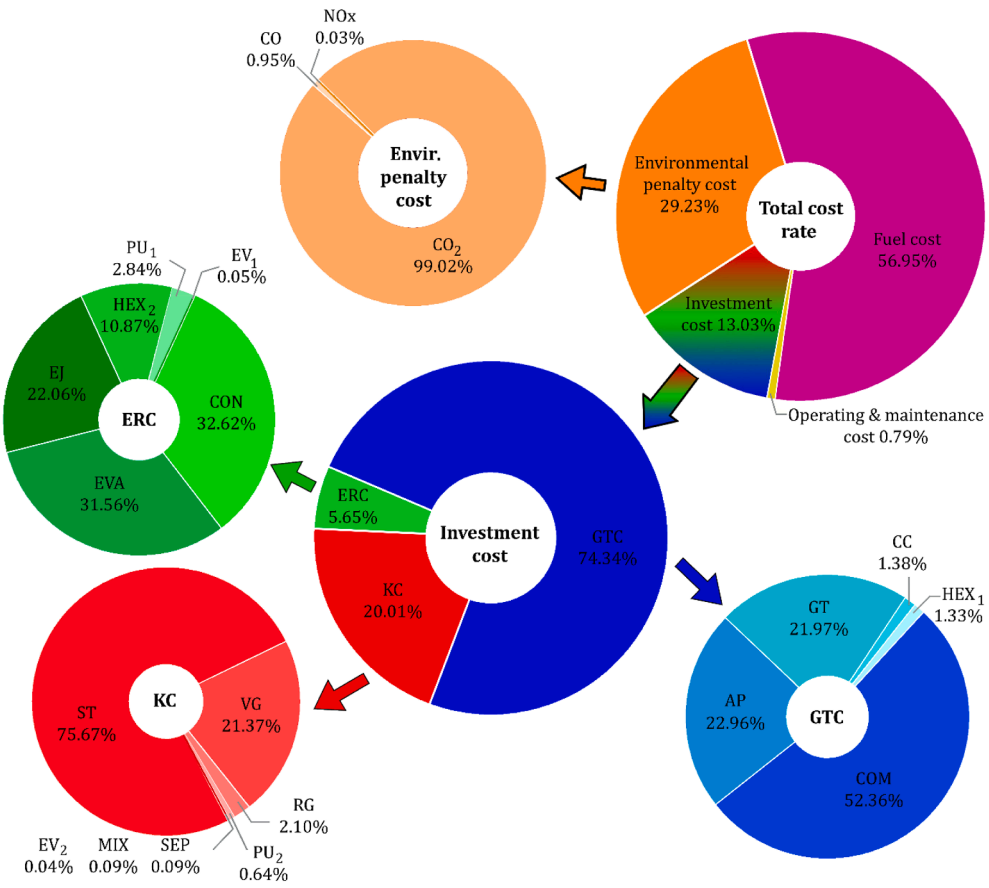

Fig. 7. Contribution of all the influential environmental and economic indices in the total cost rate of the TDES.

Table 9
Major outputs and evaluation criteria of the TDES.

Criteria	Symbol	Value
Produced cold	$\dot{Q}_c$	87.72 kW
Produced heat	$\dot{Q}_h$	954.48 kW
Net generated power	$\dot{W}_{net}$	1025.25 kW
Primary energy ratio	PER	61.41%
Total exergy destruction rate	$\dot{E}_{D,tot}$	2309.90 kW
Exergetic efficiency	η_{ex}	31.41%
Heat cost	c_c	58.05 $/GJ
Cold cost	c_h	7.67 $/GJ
Net power cost	c_p	161.01 $/GJ
Exergoeconomic criterion	$\dot{E}x_{eco}$	87.88 $/GJ
Exergoenvironmental criterion	$\dot{E}x_{env}$	67.94 kg/GJ

(Figs. 10–13).

(1) As the mover cycle of the proposed TDES, the design parameters of the RGTC play the main rule in performance of the system. Discussion around the effects of the RGTC's design parameters (i.e. PR_{COM} and T_{GT}) on the defined performance criteria can be expressed as follows:

- Based on the system's operating conditions, the results illustrated that increasing PR_{COM} results in the increment of system's produced cold, heat, and power. On the other side, analyzing the results showed selecting a COM with higher compression ratios results in a hotter air entering into the CC and it reduces the system's fuel consumption. Taking into account these descriptions and Eq. (6), PER continuously increases as PR_{COM} gets higher. But for η_{ex}, the increment trend is reversed after a certain value of PR_{COM}. It means that η_{ex} is maximised at a certain PR_{COM}. Also, the outputs of the modeling procedure reveal that 39.05% and 46.48% reduction occur in $\dot{E}x_{eco}$ and $\dot{E}x_{env}$ criteria as PR_{COM} varies from 5 to 15.
- Increasing T_{GT} from 1200 K to 1400 K leads to 14.10% reduction of PER and 1.69% increment of η_{ex}. Also, higher values of T_{GT} appears in the lower system's total cost rate and pollutant emissions. On the other side, the exergy of productions is also reduced by increasing T_{GT}. Due to higher order-of-magnitude for reduction of produced exergy compared to reduction of costs and emissions, the exergoeconomic and exergoenvironmental criteria are reduced as T_{GT} gets higher.

(2) Although the design parameters of the KC and ERC do not affect the amount of the system's emissions, they are effective in overall performance of the TDES. In the other word, this is the advantage of the exergoenvironmental analysis compared to the conventional exergetic- and environmental-alone analyses. So that, variation of X_B, P_{VG}, $\Delta T_{PP,HEX_2}$, and T_{EVA} within their investigated range leads up to 14.52%, 6.17%, 0.35%, and 7.00% variation of $\dot{E}x_{env}$.

(3) Comparing these figures proves that the highest and lowest changes in system's evaluation criteria are related to PR_{COM} and $\Delta T_{PP,HEX_2}$. It means that the system performance has the highest and lowest sensitivity on the variation of PR_{COM} and $\Delta T_{PP,HEX_2}$, respectively.

(4) The following tips describe how the design parameters affect the system's evaluation criteria:

- Among all of the investigated design parameters, all of them have a same impact on $\dot{E}x_{eco}$ and $\dot{E}x_{env}$ criteria, except $\Delta T_{PP,HEX_2}$. So

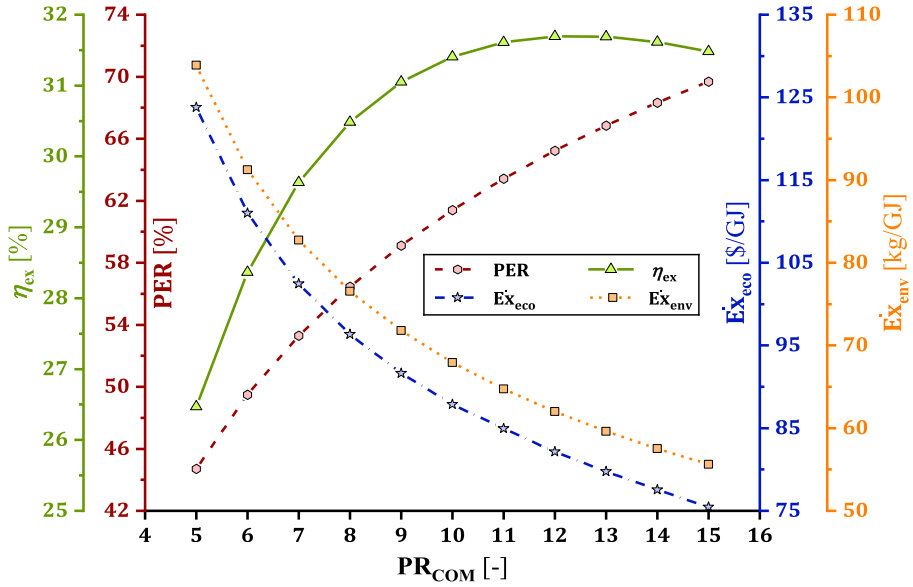

Fig. 8. The effect of pressure ratio of compressor on the primary energy ratio, exergetic efficiency, exergoeconomic criterion, and exergoenvironmental criterion.

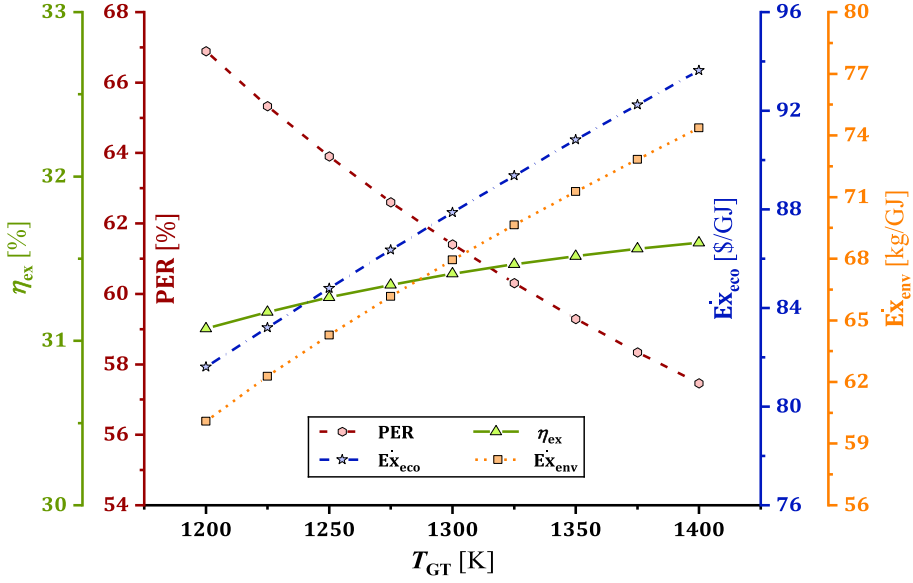

Fig. 9. The effect of inlet temperature of gas turbine on the primary energy ratio, exergetic efficiency, exergoeconomic criterion, and exergoenvironmental criterion.

that, increasing PR_{COM}, reducing T_{GT}, increasing X_B, reducing P_{VG}, and increasing T_{EVA} reduces both of the $\dot{E}x_{eco}$ and $\dot{E}x_{env}$. While, increasing and reducing $\Delta T_{PP,HEX_2}$ leads to reduction of $\dot{E}x_{eco}$ and $\dot{E}x_{env}$ criteria.

- Increasing PR_{COM}, reducing T_{GT}, increasing X_B, reducing P_{VG}, reducing $\Delta T_{PP,HEX_2}$, and increasing T_{EVA} results in a higher PER.
- For η_{ex}, variation of PR_{COM}, X_B, and P_{VG} causes creation of a certain point in which the maximum amount of η_{ex} is observed.

But for the other design parameter, the results illustrate that increasing T_{GT}, reducing $\Delta T_{PP,HEX_2}$, and increasing T_{EVA} leads to increment of η_{ex}.

- Taking into account the previous points, it can be inferred that there are various interactions between conflicting objectives. In such conditions, the needs for a multi-objective optimisation procedure is sensed to achieve optimal conditions at which all of the defined evaluation criterion be at their best possible values simultaneously.

7.3. Results of the optimisation procedure

The Pareto front obtained by NSGA-II is illustrated in Fig. 14a. Also, for a better demonstration, different two-dimensional views of the Pareto front is also depicted in Fig. 14b–d. As can be seen, none of Pareto's results dominates the other. Each of the points in the Pareto front could be considered as an optimal solution. Hence, a decision-making method should be used for selecting the appropriate point based on the design requirements. The final optimal solution selected by LINMAP decision-making method is given in Table 10.

The scatter distribution for the design parameters of the proposed TDES given in Fig. 15. As depicted in this figure, scatter distribution presents a suitable visual overview of the results, obtained by NSGA-II, related to the design parameter of the last population in the feasible set.

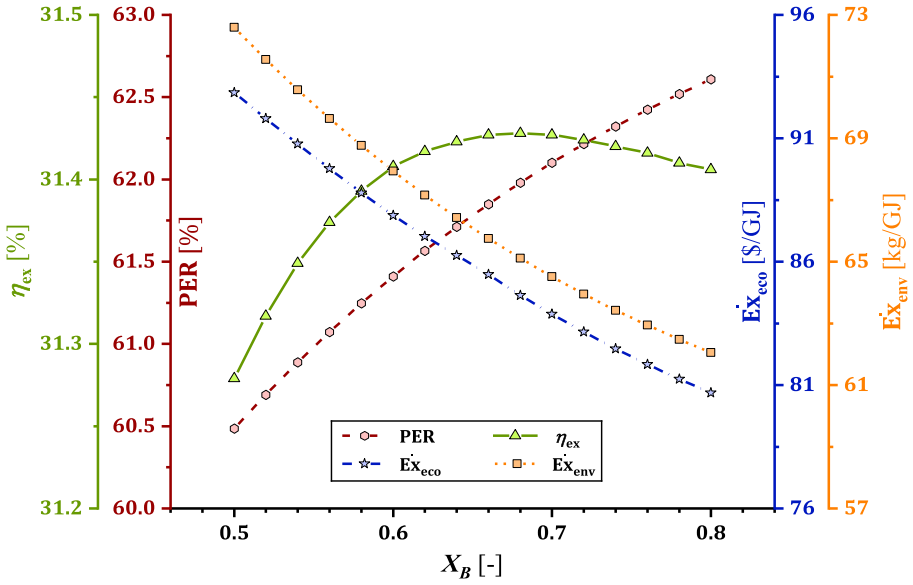

Fig. 10. The effect of ammonia mass fraction in basic AWM on the primary energy ratio, exergetic efficiency, exergoeconomic criterion, and exergoenvironmental criterion.

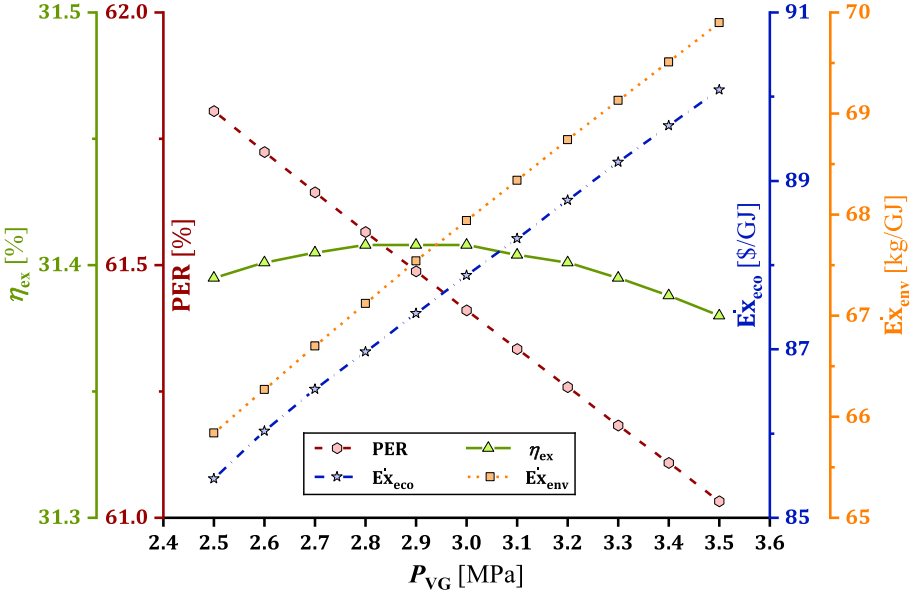

Fig. 11. The effect of pressure of vapor generator on the primary energy ratio, exergetic efficiency, exergoeconomic criterion, and exergoenvironmental criterion.

It can be seen that all results are within the allowable range. For design parameters of PR_{COM}, X_B and T_{EVA}, the majority of the results have been obtained nearby upper bound. This issue has occurred in the vicinity of lower bound for T_{GT}. But the results obtained for parameters P_{VG} and $\Delta T_{PP,HEX_2}$ are located in a wider range of their allowable range. This issue represents an important result in optimisation theory. It is the sensitivity of the problem evaluation criteria to the design parameters. Actually, the influence of the design parameters P_{VG} and $\Delta T_{PP,HEX_2}$ on the evaluation criteria is lower than the other variables. This issue has caused the population members of the optimisation algorithm converge to different results with high scattering for these two variables.

8. Concluding remarks and perspective

In this work, a novel trigeneration district energy system (TDES) was designed which comprises an RGTC, a KC, and an ER cycles. The TDES acts as a monolithic CCHP plant. The two powerful approaches of the exergoeconomic and exergoenvironmental analyses are applied for evaluating the system's performance. Four performance evaluation criteria are defined: primary energy ratio, PER, exergetic efficiency (η_{ex}), exergoeconomic criterion ($\dot{E}x_{eco}$), and exergoenvironmental criterion ($\dot{E}x_{env}$). As the final step, the optimal conditions of the design parameters and evaluation criteria were obtained by developing a powerful multi-objective optimisation program based on NSGA-II optimisation approach. The summary of the research outputs, challenges ahead, and

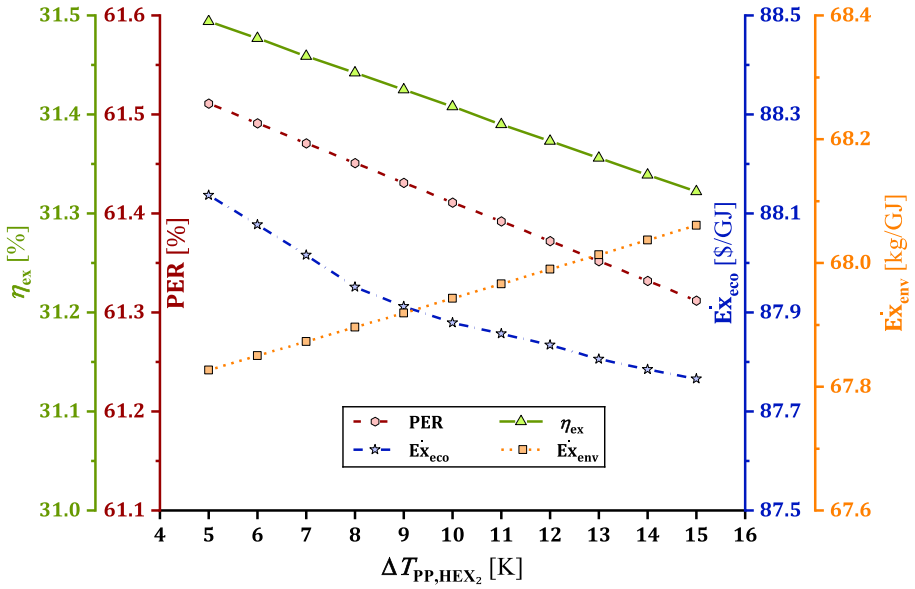

Fig. 12. The effect of pinch-point temperature difference of heat exchanger 2 on the primary energy ratio, exergetic efficiency, exergoeconomic criterion, and exergoenvironmental criterion.

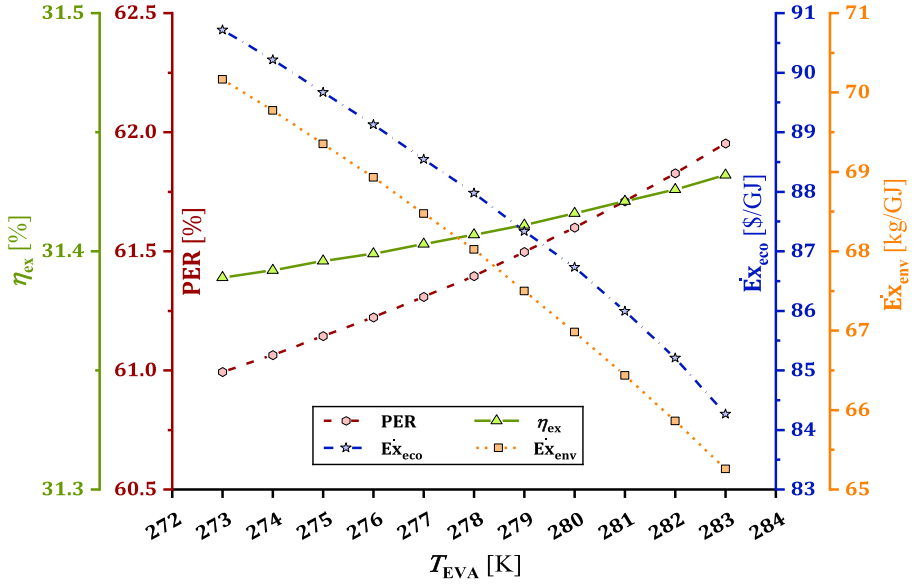

Fig. 13. The effect of temperature of evaporator on the primary energy ratio, exergetic efficiency, exergoeconomic criterion, and exergoenvironmental criterion.

the prespective of the work can be concluded as follows:

- Analyzing the exergy flow diagram of the integrated system illustrated that the combustor of the RGTC is the main source of irreversibility among all of the components. At the same conditions, the minimum rate of exergy destruction is related to pump 2 in the KC. The results of the exergoeconomic evaluation showed that the combustor and pump 2 have also the maximum and minimum cost of exergy destruction, respectively. Further, the exergetic analysis showed that the KC has a very low exergy destruction. The reason can be sought in working fluid of the KC (ammonia-water mixture) because this fluid provides a better match to the hot fluid (i.e. heat source). This can be considered as the advantage of the KC compared to other low-temperature power cycles.

After analyzing the system at the base conditions, a comprehensive parametric study was prepared for assessing the sensitivity of the evaluation criteria to the system's design parameters. This includes the pressure ratio of compressor (PR_{COM}), the inlet temperature of the gas turbine (T_{GT}), the mass fraction of ammonia in the basic ammonia-water mixture (X_B), the pressure of vapor generator (P_{VG}), the pinch-temperature of heat exchanger 2 ($\Delta T_{PP,HEX_2}$), and temperature of

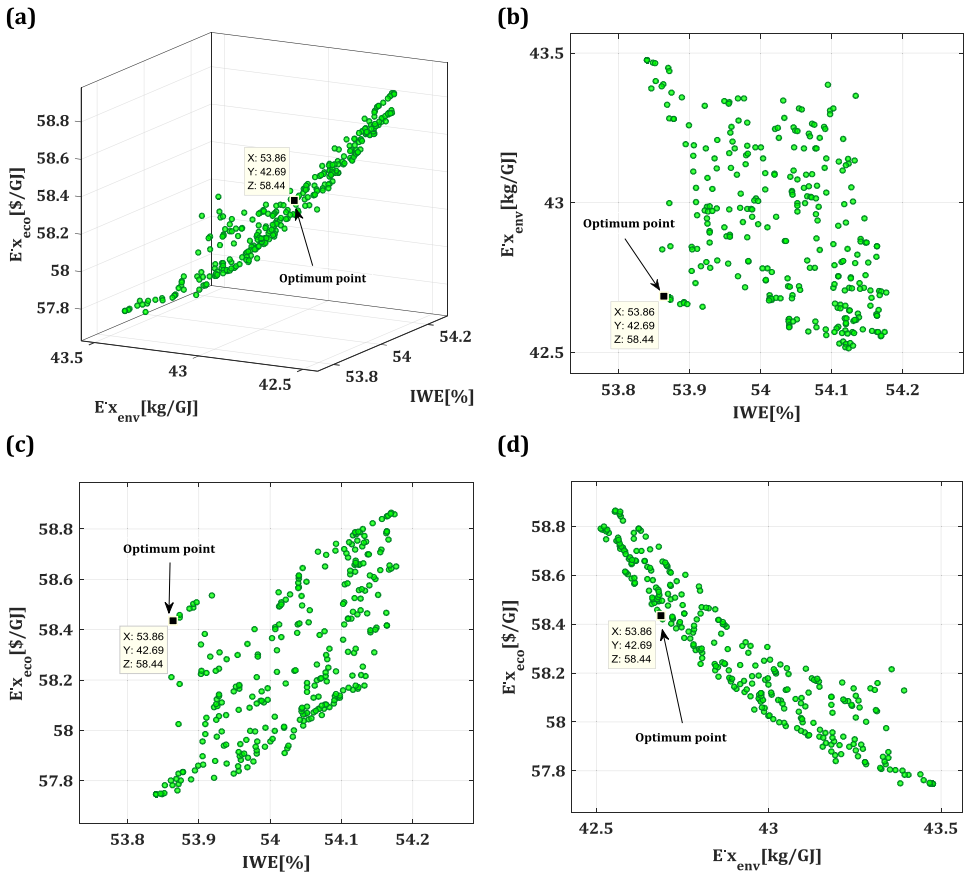

Fig. 14. Pareto frontier of the optimal solution points of the proposed TDES from four different views.

Table 10
The optimum value of the design parameters and evaluation criteria.

Item		Optimum value	
Design parameters			
PR_{COM}		14.92	
T_{GT}		1201.19 K	
X_B		0.79	
P_{VG}		2.618 MPa	
$\Delta T_{PP,HEX_2}$		12.98 K	
T_{EVA}		282.78 K	
Evaluation criteria			
IWE	PER	53.86%	76.93%
—	η_{ex}	—	30.80%
$\dot{E}x_{eco}$		58.44 $/GJ	
$\dot{E}x_{env}$		42.69 kg/GJ	

evaporator (T_{EVA}). This parametric study revealed that the highest and the lowest changes in the system's evaluation criteria is related to PR_{COM} and $\Delta T_{PP,HEX_2}$.

- Applying the optimisation procedure, it was observed that the optimum values of the evaluation criteria werePER = 76.9%, η_{ex}=30.8%, $\dot{E}x_{eco}$=58.4 $/GJ, and $\dot{E}x_{env}$ = 42.7 kg/GJ. Comparing these values with those of the base system discloses that an improvement of 25.3%, 33.5%, and 37.2% in PER, $\dot{E}x_{eco}$, and $\dot{E}x_{env}$, together with a 1.9% reduction in η_{ex} was achieved after the optimisation procedure.
- Due to the high contribution of the mover cycle to the irreversibility of the whole system, it would be a wise idea to focus on this part of the hybrid system for performance enhancement. As a suggestion, making some structural modifications in the combustion chamber (as the main source of the irreversibility) and evaluating the modifications by utilizing numerical simulations could be considered in future studies. Generally, improving the components of the mover cycle in such multi-generation systems from exergy and economic points of view are always highlighted as future possible works in this area.

Since global energy matrix is moving towards such highly integrated and multi-generation energy systems, finding the most appropriate combination of energy supplier technologies for case-specific energy systems based on the local energy regulations, availability of resources, and specific needs through comprehensive techno-economic analyses/optimisations can be the next category of future interesting works in this context. Additionally, investigating the participation of the proposed TDES in the energy market is a challengeable and interesting topic for future works. In this way, in order to achieve the optimal participation of

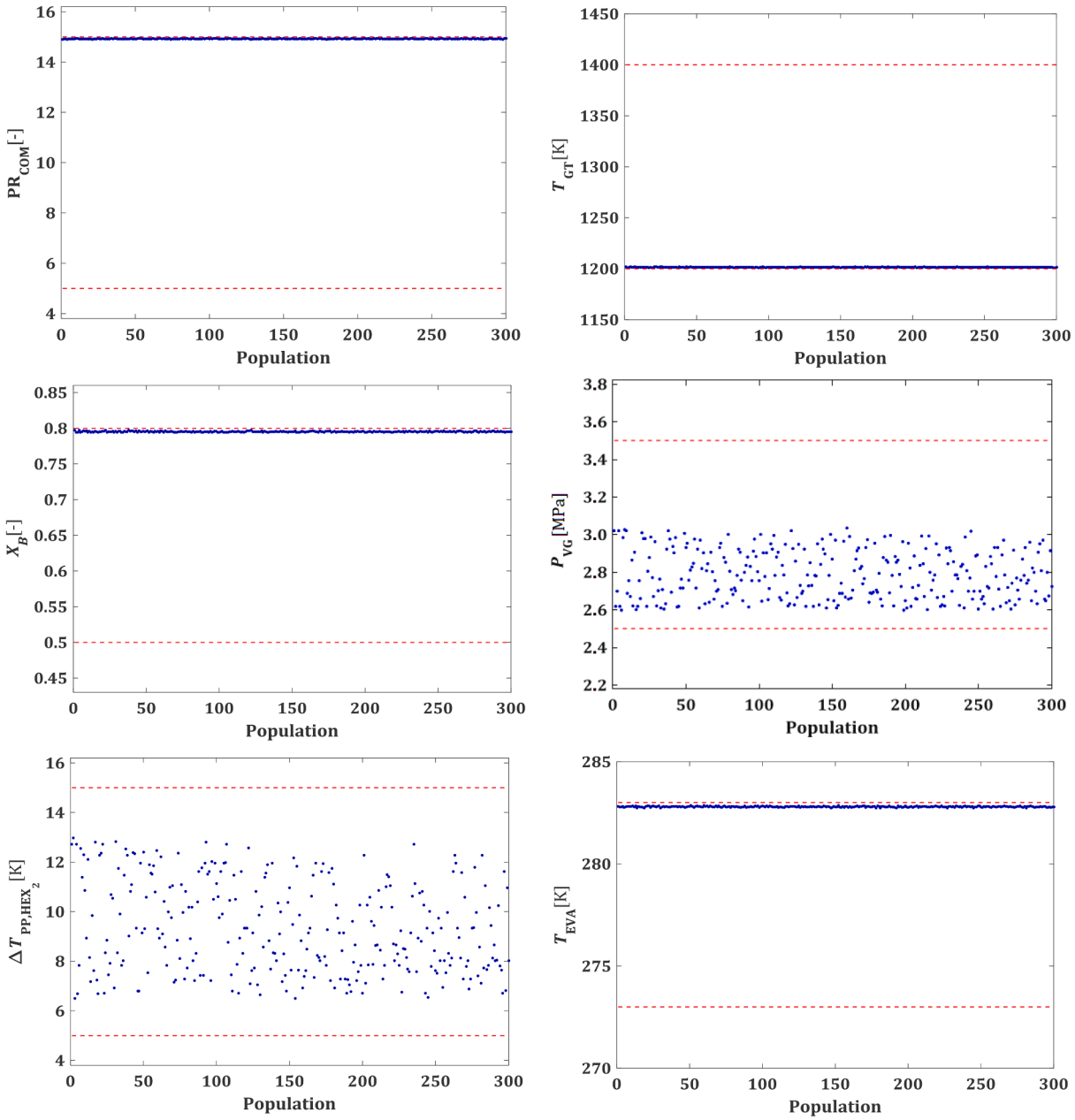

Fig. 15. Scatter distribution for the TDES design parameters.

the proposed system in a multi-energy market, we intend to present the bidding strategy problem for the CCHP system in our future work.

CRediT authorship contribution statement

Amir Ebrahimi-Moghadam: Writing - original draft, Writing - review & editing, Visualization, Methodology, Validation, Software, Investigation. **Mahmood Farzaneh-Gord:** Supervision, Project administration, Formal analysis. **Ali Jabari Moghadam:** Supervision, Project administration, Formal analysis. **Nidal H. Abu-Hamdeh:** Writing - review & editing, Funding acquisition. **Mohammad Ali Lasemi:** Methodology, Software, Formal analysis. **Ahmad Arabkoohsar:** Supervision, Writing - review & editing. **Ashkan Alimoradi:** Writing - review & editing.

Declaration of Competing Interest

The authors declare that they have no known competing financial interests or personal relationships that could have appeared to influence the work reported in this paper.

Acknowledgments

The Deanship of Scientific Research (DSR) at King Abdulaziz University, Jeddah, Saudi Arabia funded this project, under grant no. (FP-42-42).

Table A1
Details of the energy balance equation and fuel and product exergies definition for the system components.

Component	Energy balance	Fuel and product exergies	
		Fuel exergy ($\dot{E}_F$)	Product exergy ($\dot{E}_P$)
COM	$\dot{W}_{COM} = \dot{m}_1(h_2 - h_1), \eta_{COM,is} = \frac{h_{2,is} - h_1}{h_2 - h_1}$	$\dot{W}_{COM}$	$\dot{E}_2 - \dot{E}_1$
AP	$\dot{Q}_{AP} = \dot{m}_2(h_3 - h_2) = \dot{m}_5(h_5 - h_6)$	$\dot{E}_5 - \dot{E}_6$	$\dot{E}_3 - \dot{E}_2$
CC	$\dot{m}_3 h_3 + \dot{m}_{10} \times LHV = \dot{m}_4 h_4 + (1 - \eta_{CC})\dot{m}_{10} \times LHV$	$\dot{E}_3 + \dot{E}_{10}$	$\dot{E}_4$
GT	$\dot{W}_{GT} = \dot{m}_5(h_4 - h_5), \eta_{GT,is} = \frac{h_4 - h_5}{h_4 - h_{5,is}}$	$\dot{E}_4 - \dot{E}_5$	$\dot{W}_{GT}$
HEX_1	$\dot{Q}_{HEX_1} = \dot{m}_7(h_6 - h_7) = \dot{m}_8(h_9 - h_8)$	$\dot{E}_6 - \dot{E}_7$	$\dot{E}_9 - \dot{E}_8$
EJ	Refer to Table A2	$\dot{E}_{12} + \dot{E}_{13}$	$\dot{E}_{14}$
EVA	$\dot{Q}_{EVA} = \dot{m}_{13}(h_{13} - h_{19}) = \dot{m}_{32}(h_{32} - h_{33})$	$\dot{E}_{19} - \dot{E}_{13}$	$\dot{E}_{33} - \dot{E}_{32}$
CON	$\dot{Q}_{CON} = \dot{m}_{14}(h_{14} - h_{15}) = \dot{m}_{30}(h_{31} - h_{30})$	$\dot{E}_{14} - \dot{E}_{15}$	$\dot{E}_{31} - \dot{E}_{30}$
EV_1	$h_{19} = h_{17}$	$\dot{E}_{17}$	$\dot{E}_{19}$
PU_1	$\dot{W}_{PU_1} = \dot{m}_{16}(h_{18} - h_{16}), \eta_{PU_1,is} = \frac{h_{18,is} - h_{16}}{h_{18} - h_{16}}$	$\dot{W}_{PU_1}$	$\dot{E}_{18} - \dot{E}_{16}$
VG	$\dot{Q}_{VG} = \dot{m}_{11}(h_7 - h_{11}) = \dot{m}_{20}(h_{20} - h_{29})$	$\dot{E}_7 - \dot{E}_{11}$	$\dot{E}_{20} - \dot{E}_{29}$
SEP	$\dot{m}_{20} h_{20} = \dot{m}_{21} h_{21} + \dot{m}_{23} h_{23}$	$\dot{E}_{20}$	$\dot{E}_{21} + \dot{E}_{23}$
RG	$\dot{Q}_{RG} = \dot{m}_{28}(h_{29} - h_{28}) = \dot{m}_{23}(h_{23} - h_{24})$	$\dot{E}_{23} - \dot{E}_{24}$	$\dot{E}_{29} - \dot{E}_{28}$
EV_2	$h_{25} = h_{24}$	$\dot{E}_{24}$	$\dot{E}_{25}$
MIX	$\dot{m}_{26} h_{26} = \dot{m}_{25} h_{25} + \dot{m}_{22} h_{22}$	$\dot{E}_{22} + \dot{E}_{25}$	$\dot{E}_{26}$
ST	$\dot{W}_{ST} = \dot{m}_{22}(h_{21} - h_{22}), \eta_{ST,is} = \frac{h_{21} - h_{22}}{h_{21} - h_{22,is}}$	$\dot{E}_{13} - \dot{E}_{14}$	$\dot{W}_{ST}$
HEX_2	$\dot{Q}_{HEX_2} = \dot{m}_{26}(h_{26} - h_{27}) = \dot{m}_{18}(h_{12} - h_{18})$	$\dot{E}_{26} - \dot{E}_{27}$	$\dot{E}_{12} - \dot{E}_{18}$
PU_2	$\dot{W}_{PU_2} = \dot{m}_{27}(h_{28} - h_{27}), \eta_{PU_2,is} = \frac{h_{28,is} - h_{27}}{h_{28} - h_{27}}$	$\dot{W}_{PU_2}$	$\dot{E}_{28} - \dot{E}_{27}$

Table A2
Details of the required equations for energetic modeling of the EJ.

Equation name	Formulation
Mass entrainment ratio of the EJ	$\mu = \frac{\dot{m}_{SF}}{\dot{m}_{PF}}$
Energy conservation in the nozzle for the PF	$V_{PF,N_{out}} = \sqrt{2(h_{PF,N_{in}} - h_{PF,N_{out}})}$
Isentropic efficiency of the nozzle	$\eta_{N,is} = \frac{h_{PF,N_{in}} - h_{PF,N_{out}}}{h_{PF,N_{in}} - h_{PF,N_{out},is}}$
Energy conservation in the nozzle for the SF	$V_{SF,N_{out}} = \sqrt{2(h_{SF,N_{in}} - h_{SF,N_{out}})}$
Momentum conservation for the mixing chamber	$V_{MF,is} = \frac{V_{PF,N_{out}} + \mu V_{SF,N_{out}}}{1 + \mu}$
Efficiency of the mixing chamber	$\eta_M = \frac{V_{MF}^2}{V_{MF,is}^2}$
Energy conservation for the mixing chamber	$h_{MF} = \frac{h_{PF,N_{out}} + \mu h_{SF}}{1 + \mu} - \frac{V_{MF}^2}{2}$
Isentropic efficiency of the diffuser	$\eta_{D,is} = \frac{h_{D,is} - h_{MF}}{h_D - h_{MF}}$
Mass entrainment ratio of the EJ based on the EJ's parameters	$\mu = \sqrt{\eta_{N,is}\eta_M\eta_{D,is}(h_{PF,N_{in}} - h_{PF,N_{out},is})/(h_{D,is} - h_{MF})} - 1$

Appendix A. The required details for energetic and exergetic modeling procedure (thermodynamic modeling)

This appendix presents details about the energetic and exergetic modeling procedure. Due to the negligible changes in the height, variation of the potential energy at the inlet and outlet of all system components are neglected. Also, changes in the velocity kinetic at the inlet and outlet of all system components are negligible except the EJ. Hence, variation of the kinetic energy at the inlet and outlet of all system components are neglected except the EJ. The final format of the required equations for energetic and exergetic analysis is listed in Tables A1 and A2. It should be noted that, a one-dimensional flow is assumed for the EJ modeling and the EJ walls are adiabatic. Also, the losses due to the mixing and fluid flow within the EJ are applied by considering efficiencies of $\eta_{N,is}$, η_M, and $\eta_{D,is}$ for nozzle, mixing chamber, and diffuser, respectively.

Appendix B. The required details for the exergoeconomic modeling procedure

The purchase cost of the system's equipment can be estimated using the functions presented in Table B1 [51,60,61]. The notable point is that these costs should be updated from their development year to the current year. Here, this process is done by using Eq. (B1) through yearly averaged chemical engineering plant cost index (CEPCI).

$$Z_{2019} = Z_{DY} \times \left[\frac{CEPCI_{2019}}{CEPCI_{DY}}\right] \tag{B1}$$

Table B1
System's purchasing equipment cost functions.

Component	Purchase equipment cost [$]	Year of development	CEPCI
COM	$Z_{COM} = \left(\frac{39.5\times\dot{m}_1}{0.9-\eta_{COM,is}}\right)\left(\frac{P_2}{P_1}\right)\left[\ln\left(\frac{P_2}{P_1}\right)\right]$	1994	368.1
AP	$Z_{AP} = 2290\times(A_{AP})^{0.6}$	1994	368.1
CC	$Z_{CC} = \left(\frac{25.6\times\dot{m}_3}{0.995-\frac{P_4}{P_3}}\right)[1+\exp(0.018T_4-26.4)]$	1994	368.1
GT	$Z_{GT} = \left(\frac{266.3\times\dot{m}_4}{0.92-\eta_{GT,is}}\right)\left[\ln\left(\frac{P_4}{P_5}\right)\right][1+\exp(0.036T_4-54.4)]$	1994	368.1
HEX_1	$Z_{HEX_1} = 130\times\left(\frac{A_{HEX_1}}{0.093}\right)^{0.78}$	2000	394.1
EJ	$Z_{EJ} = 1000\times16.14\times0.989\times\dot{m}_{12}\times\left(\frac{T_{12}}{0.1P_{12}}\right)^{0.05}\times(0.1P_{14})^{-0.75}$	2001	394.3
EVA	$Z_{EVA} = 16000\times\left(\frac{A_{EVA}}{100}\right)^{0.6}$	2000	394.1
CON	$Z_{CON} = 8000\times\left(\frac{A_{CON}}{100}\right)^{0.6}$	2000	394.1
EVs	$Z_{EV} = 114.5\times\dot{m}_{EV}$	2000	394.1
PUs	$Z_{PU} = 2100\left(\frac{\dot{W}_{PU}}{10}\right)^{0.26}\times\left(\frac{1-\eta_{PU,is}}{\eta_{PU,is}}\right)^{0.5}$	2000	394.1
VG	$Z_{VG} = (309.143\times A_{VG})+231.915$	2000	394.1
Separator	$Z_{SEP} = 114.5\times\left(\dot{m}_{20}\right)^{0.67}$	2000	394.1
RG	$Z_{RG} = 12000\times\left(\frac{A_{RG_2}}{100}\right)^{0.6}$	2000	394.1
MIX	$Z_{MIX} = 114.5\times\left(\dot{m}_{26}\right)^{0.67}$	2000	394.1
ST	$Z_{ST} = 3880.5\times\dot{W}_{ST}^{0.7}\left(1+\left(\frac{0.05}{1-\eta_{ST,is}}\right)^3\right)\left[1+5\exp\left(\frac{T_{21}-866}{10.42}\right)\right]$	2003	402
HEX_2	$Z_{HEX_2} = 12000\left(\frac{A_{HEX_2}}{100}\right)^{0.6}$	2000	394.1

in which, the index of DY refers to the development year of the cost function. Also, the newest available CEPCI is related to the year of 2019 which is equal to$CEPCI_{2019} = 607.5$ [61].

Appendix C. The required details for the exergoenvironmental modeling procedure

The required parameters and constants of Eq. (23) in exergoenvironmental modeling procedure can be achieved using Eqs. (C1)–(C3) and Table C1 [17].

$$\delta = \begin{cases} \varnothing; & \varnothing < 1 \\ \varnothing - 0.7; & \varnothing \geq 1 \end{cases} \tag{C1}$$

$$\varnothing = \frac{(FA)_{actual}}{(FA)_{stoichiometric}} \tag{C2}$$

$$\begin{cases} x^* = a_1 + b_1\delta + c_1\delta^2 \\ y^* = a_2 + b_2\delta + c_2\delta^2 \\ z^* = a_3 + b_3\delta + c_3\delta^2 \end{cases} \tag{C3}$$

Table C1
The required constants in exergoenvironmental modeling procedure.

$1\leq\varnothing\leq1.6$		$0.3\leq\varnothing<1$		Constant
$2\leq\Theta\leq3.2$	$0.92\leq\Theta<2$	$2\leq\Theta\leq3.2$	$0.92\leq\Theta<2$	
1246.1778	916.8261	2315.752	2361.7644	$\mathscr{C}$
0.3819	0.2885	−0.0493	0.1157	κ
0.3479	0.1456	−1.1141	−0.9489	ϑ
−2.0365	−3.2771	−1.1807	−1.0976	ε
0.0361	0.0311	0.0106	0.0143	a_1
−0.085	−0.078	−0.045	−0.0553	b_1
0.0517	0.0497	0.0482	0.0526	c_1
0.0097	0.0254	0.5688	0.3955	a_2
0.502	0.2602	−0.55	−0.4417	b_2
−0.2471	−0.1318	0.1319	0.141	c_2
0.017	0.0042	0.0108	0.0052	a_3
−0.1894	−0.1781	−0.1291	−0.1289	b_3
0.1037	0.098	0.0848	0.0827	c_3

References

[1] Vujanović M, Wang Q, Mohsen M, Duić N, Yan J. Sustainable energy technologies and environmental impacts of energy systems. Appl Energy 2019;256:113919. https://doi.org/10.1016/j.apenergy.2019.113919.

[2] Nikzad A, Chahartaghi M, Ahmadi MH. Technical, economic, and environmental modeling of solar water pump for irrigation of rice in Mazandaran province in Iran: a case study. J Clean Prod 2019;239:118007. https://doi.org/10.1016/j.jclepro.2019.118007.

[3] Balakheli MM, Chahartaghi M, Sheykhi M, Hashemian SM, Rafiee N. Analysis of different arrangements of combined cooling, heating and power systems with internal combustion engine from energy, economic and environmental viewpoints. Energy Convers Manag 2020;203:112253. https://doi.org/10.1016/j.enconman.2019.112253.

[4] Ebadollahi M, Rostamzadeh H, Pedram MZ, Ghaebi H, Amidpour M. Proposal and assessment of a new geothermal-based multigeneration system for cooling, heating, power, and hydrogen production, using LNG cold energy recovery. Renew Energy 2019;135:66–87. https://doi.org/10.1016/j.renene.2018.11.108.

[5] Chahartaghi M, Sheykhi M. Energy, environmental and economic evaluations of a CCHP system driven by Stirling engine with helium and hydrogen as working gases. Energy 2019;174:1251–66. https://doi.org/10.1016/j.energy.2019.03.012.

[6] Arabkoohsar A. Combination of air-based high-temperature heat and power storage system with an Organic Rankine Cycle for an improved electricity efficiency. Appl Therm Eng 2020;167:114762. https://doi.org/10.1016/j.applthermaleng.2019.114762.

[7] Owebor K, Oko COC, Diemuodeke EO, Ogorure OJ. Thermo-environmental and economic analysis of an integrated municipal waste-to-energy solid oxide fuel cell, gas-, steam-, organic fluid- and absorption refrigeration cycle thermal power plants. Appl Energy 2019;239:1385–401. https://doi.org/10.1016/j.apenergy.2019.02.032.

[8] Du Y, Fan G, Zheng S, Zhao P, Wang J, Dai Y. Novel operation strategy for a gas turbine and high-temperature KCS combined cycle. Energy Convers Manag 2020;217:113000. https://doi.org/10.1016/j.enconman.2020.113000.

[9] Gholizadeh T, Vajdi M, Mohammadkhani F. Thermodynamic and thermoeconomic analysis of basic and modified power generation systems fueled by biogas. Energy Convers Manag 2019;181:463–75. https://doi.org/10.1016/j.enconman.2018.12.011.

[10] Singh OK. Performance enhancement of combined cycle power plant using inlet air cooling by exhaust heat operated ammonia-water absorption refrigeration system. Appl Energy 2016;180:867–79. https://doi.org/10.1016/j.apenergy.2016.08.042.

[11] Cao Y, Gao Y, Zheng Y, Dai Y. Optimum design and thermodynamic analysis of a gas turbine and ORC combined cycle with recuperators. Energy Convers Manag 2016;116:32–41. https://doi.org/10.1016/j.enconman.2016.02.073.

[12] Wang X, Dai Y. Exergoeconomic analysis of utilizing the transcritical CO2 cycle and the ORC for a recompression supercritical CO2 cycle waste heat recovery: a comparative study. Appl Energy 2016;170:193–207. https://doi.org/10.1016/j.apenergy.2016.02.112.

[13] Zare V, Mahmoudi SMS. A thermodynamic comparison between organic Rankine and Kalina cycles for waste heat recovery from the Gas Turbine-Modular Helium Reactor. Energy 2015;79:398–406. https://doi.org/10.1016/j.energy.2014.11.026.

[14] Gholizadeh T, Vajdi M, Rostamzadeh H. A new biogas-fueled bi-evaporator electricity/cooling cogeneration system: exergoeconomic optimization. Energy Convers Manag 2019;196:1193–207. https://doi.org/10.1016/j.enconman.2019.06.053.

[15] Xia J, Wang J, Lou J, Zhao P, Dai Y. Thermo-economic analysis and optimization of a combined cooling and power (CCP) system for engine waste heat recovery. Energy Convers Manag 2016;128:303–16. https://doi.org/10.1016/j.enconman.2016.09.086.

[16] Ebrahimi-Moghadam A, Moghadam AJ, Farzaneh-Gord M. Comprehensive techno-economic and environmental sensitivity analysis and multi-objective optimization of a novel heat and power system for natural gas city gate stations. J Clean Prod 2020;262:121261. https://doi.org/10.1016/j.jclepro.2020.121261.

[17] Ebrahimi-Moghadam A, Moghadam AJ, Farzaneh-Gord M, Aliakbari K. Proposal and assessment of a novel combined heat and power system: energy, exergy, environmental and economic analysis. Energy Convers Manag 2020;204:112307. https://doi.org/10.1016/j.enconman.2019.112307.

[18] Shokouhi Tabrizi AH, Niazmand H, Farzaneh-Gord M, Ebrahimi-Moghadam A. Energy, exergy and economic analysis of utilizing the supercritical CO2 recompression Brayton cycle integrated with solar energy in natural gas city gate station. J Therm Anal Calorim 2020. https://doi.org/10.1007/s10973-020-10241-9.

[19] Kim MJ, Kim TS, Flores RJ, Brouwer J. Neural-network-based optimization for economic dispatch of combined heat and power systems. Appl Energy 2020;265:114785. https://doi.org/10.1016/j.apenergy.2020.114785.

[20] Wang Z, Han W, Zhang N, Su B, Gan Z, Jin H. Effects of different alternative control methods for gas turbine on the off-design performance of a trigeneration system. Appl Energy 2018;215:227–36. https://doi.org/10.1016/j.apenergy.2018.01.053.

[21] Moghimi M, Emadi M, Mirzazade Akbarpoor A, Mollaei M. Energy and exergy investigation of a combined cooling, heating, power generation, and seawater desalination system. Appl Therm Eng 2018;140:814–27. https://doi.org/10.1016/j.applthermaleng.2018.05.092.

[22] Ebrahimi M, Majidi S. Exergy-energy-environ evaluation of combined cooling heating and power system based on a double stage compression regenerative gas turbine in large scales. Energy Convers Manag 2017;150:122–33. https://doi.org/10.1016/j.enconman.2017.08.004.

[23] Ebrahimi M, Ahookhosh K. Integrated energy–exergy optimization of a novel micro-CCHP cycle based on MGT–ORC and steam ejector refrigerator. Appl Therm Eng 2016;102:1206–18. https://doi.org/10.1016/j.applthermaleng.2016.04.015.

[24] Xu XX, Liu C, Fu X, Gao H, Li Y. Energy and exergy analyses of a modified combined cooling, heating, and power system using supercritical CO2. Energy 2015;86:414–22. https://doi.org/10.1016/j.energy.2015.04.043.

[25] Wu C, Xu X, Li Q, Li J, Wang S, Liu C. Proposal and assessment of a combined cooling and power system based on the regenerative supercritical carbon dioxide Brayton cycle integrated with an absorption refrigeration cycle for engine waste heat recovery. Energy Convers Manag 2020;207:112527. https://doi.org/10.1016/j.enconman.2020.112527.

[26] Li Y, Liu Y, Zhang G, Yang Y. Thermodynamic analysis of a novel combined cooling and power system utilizing liquefied natural gas (LNG) cryogenic energy and low-temperature waste heat. Energy 2020;199:117479. https://doi.org/10.1016/j.energy.2020.117479.

[27] Tańczuk M, Skorek J, Bargiel P. Energy and economic optimization of the repowering of coal-fired municipal district heating source by a gas turbine. Energy Convers Manag 2017;149:885–95. https://doi.org/10.1016/j.enconman.2017.03.053.

[28] Ganjehkaviri A, Mohd Jaafar MN, Ahmadi P, Barzegaravval H. Modelling and optimization of combined cycle power plant based on exergoeconomic and environmental analyses. Appl Therm Eng 2014;67:566–78. https://doi.org/10.1016/j.applthermaleng.2014.03.018.

[29] Majdi Yazdi MR, Ommi F, Ehyaei MA, Rosen MA. Comparison of gas turbine inlet air cooling systems for several climates in Iran using energy, exergy, economic, and environmental (4E) analyses. Energy Convers Manag 2020;216:112944. https://doi.org/10.1016/j.enconman.2020.112944.

[30] Barzegaravval H, Hosseini SE, Wahid MA, Saat A Bin. Dimensionless exergo-economic and emission parameters for biogas fueled gas turbine optimization. J Clean Prod 2020;262:121153. https://doi.org/https://doi.org/10.1016/j.jclepro.2020.121153.

[31] Bonforte G, Buchgeister J, Manfrida G, Petela K. Exergoeconomic and exergoenvironmental analysis of an integrated solar gas turbine/combined cycle power plant. Energy 2018;156:352–9. https://doi.org/10.1016/j.energy.2018.05.080.

[32] Chen Y, Wang M, Liso V, Samsatli S, Samsatli NJ, Jing R, et al. Parametric analysis and optimization for exergoeconomic performance of a combined system based on solid oxide fuel cell-gas turbine and supercritical carbon dioxide Brayton cycle. Energy Convers Manag 2019;186:66–81. https://doi.org/10.1016/j.enconman.2019.02.036.

[33] Anvari S, Mahian O, Taghavifar H, Wongwises S, Desideri U. 4E analysis of a modified multigeneration system designed for power, heating/cooling, and water desalination. Appl Energy 2020;270:115107. https://doi.org/10.1016/j.apenergy.2020.115107.

[34] Nami H, Mahmoudi SMS, Nemati A. Exergy, economic and environmental impact assessment and optimization of a novel cogeneration system including a gas turbine, a supercritical CO2 and an organic Rankine cycle (GT-HRSG/SCO2). Appl Therm Eng 2017;110:1315–30. https://doi.org/10.1016/j.applthermaleng.2016.08.197.

[35] Emadi MA, Chitgar N, Oyewunmi OA, Markides CN. Working-fluid selection and thermoeconomic optimisation of a combined cycle cogeneration dual-loop organic Rankine cycle (ORC) system for solid oxide fuel cell (SOFC) waste-heat recovery. Appl Energy 2020;261:114384. https://doi.org/10.1016/j.apenergy.2019.114384.

[36] Moghimi M, Emadi M, Ahmadi P, Moghadasi H. 4E analysis and multi-objective optimization of a CCHP cycle based on gas turbine and ejector refrigeration. Appl Therm Eng 2018;141:516–30. https://doi.org/10.1016/j.applthermaleng.2018.05.075.

[37] Wang J, Lu Z, Li M, Lior N, Li W. Energy, exergy, exergoeconomic and environmental (4E) analysis of a distributed generation solar-assisted CCHP (combined cooling, heating and power) gas turbine system. Energy 2019;175:1246–58. https://doi.org/10.1016/j.energy.2019.03.147.

[38] Enayatizade H, Chahartaghi M, Hashemian SM, Arjomand A, Ahmadi MH. Techno-economic evaluation of a new CCHP system with a hydrogen production unit. Int J Low-Carbon Technol 2019;14:170–86. https://doi.org/10.1093/ijlct/ctz017.

[39] Ebrahimi-Moghadam A, Deymi-Dashtebayaz M, Jafari H, Niazmand A. Energetic, exergetic, environmental and economic assessment of a novel control system for indirect heaters in natural gas city gate stations. J Therm Anal Calorim 2020. https://doi.org/10.1007/s10973-020-09413-4.

[40] Wang E, Yu Z. A numerical analysis of a composition-adjustable Kalina cycle power plant for power generation from low-temperature geothermal sources. Appl Energy 2016;180:834–48. https://doi.org/10.1016/j.apenergy.2016.08.032.

[41] Sadi M, Arabkoohsar A. Exergoeconomic analysis of a combined solar-waste driven power plant. Renew Energy 2019;141:883–93. https://doi.org/10.1016/j.renene.2019.04.070.

[42] Boyaghchi FA, Asgari S. A comparative study on exergetic, exergoeconomic and exergoenvironmental assessments of two internal auto-cascade refrigeration cycles.

Appl Therm Eng 2017;122:723–37. https://doi.org/10.1016/j.applthermaleng.2017.05.065.
[43] Wang W, Wang J, Lu Z, Wang S. Exergoeconomic and exergoenvironmental analysis of a combined heating and power system driven by geothermal source. Energy Convers Manag 2020;211:112765. https://doi.org/10.1016/j.enconman.2020.112765.
[44] Amiri Rad E, Kazemiani-Najafabadi P. Introducing a novel optimized Dual Fuel Gas Turbine (DFGT) based on a 4E objective function. J Clean Prod 2019;206:944–54. https://doi.org/10.1016/j.jclepro.2018.09.129.
[45] Rizk NK, Mongia HC. Semianalytical correlations for NOx, CO, and UHC emissions. J Eng Gas Turbines Power 1993;115:612–9.
[46] Habibollahzade A, Gholamian E, Behzadi A. Multi-objective optimization and comparative performance analysis of hybrid biomass-based solid oxide fuel cell/solid oxide electrolyzer cell/gas turbine using different gasification agents. Appl Energy 2019;233–234:985–1002. https://doi.org/10.1016/j.apenergy.2018.10.075.
[47] Farzaneh-Gord M, Mohseni-Gharyehsafa B, Ebrahimi-Moghadam A, Jabari-Moghadam A, Toikka A, Zvereva I. Precise calculation of natural gas sound speed using neural networks: an application in flow meter calibration. Flow Meas Instrum 2018;64:90–103. https://doi.org/10.1016/j.flowmeasinst.2018.10.013.
[48] Ebrahimi-Moghadam A, Ildarabadi P, Aliakbari K, Fadaee F. Sensitivity analysis and multi-objective optimization of energy consumption and thermal comfort by using interior light shelves in residential buildings. Renew Energy 2020;159:736–55. https://doi.org/10.1016/j.renene.2020.05.127.
[49] Lasemi MA, Assili M, Hajizadeh A. Multi-objective hydrothermal generation scheduling and fuel dispatch management considering liquid fuel dispatch network modeling. Electr Power Syst Res 2020;187:106436. https://doi.org/10.1016/j.epsr.2020.106436.
[50] Deymi-Dashtebayaz M, Akhoundi M, Ebrahimi-Moghadam A, Arabkoohsar A, Jabari Moghadam A, Farzaneh-Gord M. Thermo-hydraulic analysis and optimization of CuO/water nanofluid inside helically dimpled heat exchangers. J Therm Anal Calorim 2020. https://doi.org/10.1007/s10973-020-09398-0.
[51] Ebadollahi M, Rostamzadeh H, Pedram MZ, Ghaebi H, Amidpour M. Proposal and multi-criteria optimization of two new combined heating and power systems for the Sabalan geothermal source. J Clean Prod 2019;229:1065–81. https://doi.org/10.1016/j.jclepro.2019.05.022.
[52] Lasemi MA, Assili M, Hajizadeh A. Smart energy management of thermal power plants by considering liquid fuel dispatching system modeling. Smart Grid Conf 2018;2018:1–6. https://doi.org/10.1109/SGC.2018.8777796.
[53] Kholardi F, Assili M, Lasemi MA, Hajizadeh A. Optimal management of energy hub with considering hydrogen network. In: 2018 Int Conf Smart Energy Syst Technol, 2018, p. 1–6. https://doi.org/10.1109/SEST.2018.8495664.
[54] Ebrahimi-Moghadam A, Kowsari S, Farhadi F, Deymi-Dashtebayaz M. Thermohydraulic sensitivity analysis and multi-objective optimization of Fe3O4/H2O nanofluid flow inside U-bend heat exchangers with longitudinal strip inserts. Appl Therm Eng 2020;164:114518. https://doi.org/10.1016/j.applthermaleng.2019.114518.
[55] Bejan A, Tsatsaronis G, Moran M. Thermal design and optimization. John Wiley & Sons; 1996.
[56] Ghaebi H, Parikhani T, Rostamzadeh H, Farhang B. Proposal and assessment of a novel geothermal combined cooling and power cycle based on Kalina and ejector refrigeration cycles. Appl Therm Eng 2018;130:767–81. https://doi.org/10.1016/j.applthermaleng.2017.11.067.
[57] Huang BJ, Chang JM, Wang CP, Petrenko VA. A 1-D analysis of ejector performance. Int J Refrig 1999;22:354–64. https://doi.org/10.1016/S0140-7007(99)00004-3.
[58] Ahmadi MH, Ghazvini M, Maddah H, Kahani M, Pourfarhang S, Pourfarhang A, et al. Prediction of the pressure drop for CuO/(Ethylene glycol-water) nanofluid flows in the car radiator by means of Artificial Neural Networks analysis integrated with genetic algorithm. Phys A Stat Mech Its Appl 2020;546:124008. https://doi.org/10.1016/j.physa.2019.124008.
[59] Dincer I, Rosen MA, Ahmadi P. Modeling and optimization of cogeneration and trigeneration systems. Optim Energy Syst 2017:317–97.
[60] Valero A, Lozano MA, Serra L, Tsatsaronis G, Pisa J, Frangopoulos C, et al. CGAM problem: definition and conventional solution. Energy 1994;19:279–86. https://doi.org/10.1016/0360-5442(94)90112-0.
[61] CEPCI. The Chemical Engineering Plant Cost Index n.d. https://www.chemengonline.com.